



UNIVERSITY OF PADOVA

DEPARTMENT OF INFORMATION ENGINEERING

MASTER THESIS IN CONTROL SYSTEM ENGINEERING

MPC-BASED CENTRALISED POWER CONTROL IN POWER DISTRIBUTION SYSTEM WITH EV AND PV COORDINATION

SUPERVISOR

PROF. SANDRO ZAMPIERI
UNIVERSITY OF PADOVA

MASTER CANDIDATE

A. MOHAMED MESSILEM

STUDENT ID

2043180

MCCXXII
ACADEMIC YEAR

2022-2023

Abstract

The shift from internal combustion engine (ICE) vehicles to electric vehicles (EV) in recent times has been driven primarily by the need to reduce emissions and address climate change. EVs can be powered by electricity generated from a variety of sources, including renewable energy such as solar, wind, and hydroelectric power. This reduces the dependency on finite fossil fuels, which are contributing to climate changes. The transition to a sustainable, low-carbon energy systems requires an efficient management of electrical energy, particularly in the context of photovoltaic (PV) power generation and electric vehicle (EV) charging. Efficient management of electrical energy in both PV power generation and EV charging involves a combination of advanced technologies, policy support, and consumer participation. It is an holistic approach that aims to balance energy supply and demand, reduce carbon emissions, and ensure a sustainable energy future. Demand-response programs and time-of-use pricing systems are effective mechanisms to incentives EV owners to adjust their charging behaviour based on the availability of PV generation and overall demand of electricity. This approach optimizes energy use and grid balancing. Vehicle-to-Grid (V2G) technology is being explored as a bi-directional power flow solution, allowing EVs to supply electricity to the grid during peak demand or when PV generation is insufficient. The integration of V2G capabilities allows electric vehicles to provide grid stabilization services and support the integration of intermittent renewable energy sources. Energy management systems (EMS) play a critical role in optimizing photovoltaic generation, electric vehicle charging, and other energy resources. Using advanced algorithms and optimization techniques, EMS takes into account factors such as PV generation forecasts, electricity demand, EV charging requirements and grid constraints. The result is an intelligent energy planning mechanism that minimizes grid constraints, maximizes the use of renewable energy and reduces operating costs.

Acknowledgment

I would like to express my heartfelt gratitude to several individuals and institutions who have played an indispensable role in the successful completion of my journey.

First and foremost, I extend my deepest appreciation to my parents for their unwavering love, unending support, and constant encouragement throughout my academic pursuits. Their sacrifices and guidance have been instrumental in shaping my aspiration and achievements.

I am also immensely indebted to my supervisor, Professor Sandro Zampieri, whose expertise, mentorship, and insightful guidance have significantly enriched my research work. His dedication to academic excellence and his willingness to share his knowledge have been invaluable assets to my growth as a researcher.

Furthermore, I would like to acknowledge the staff of the University of Padova for providing a conducive environment for learning and research. Their collective efforts in maintaining the institution standards and facilitating various resources have contributed significantly to my academic development.

In conclusion, I extend my heartfelt thanks to all those who have supported and believed in me throughout this academic journey. Your contributions have been pivotal in helping me reach this milestone, and I am truly grateful for your unwavering presence in my life.

Contents

ABSTRACT	iii
ACKNOWLEDGMENT	v
LIST OF FIGURES	ix
LIST OF TABLES	xi
LISTING OF ACRONYMS	xiii
1 INTRODUCTION	1
2 LITERATURE AND REVIEW	5
2.1 Overview of power distribution system	5
2.2 EV And PV Integration In Power Distribution System	5
2.3 Centralised Power Control And MPC in Power System	9
2.4 Previous Studies	9
3 POWER DISTRIBUTION SYSTEM MODELLING	27
3.1 Battery Model	28
3.2 EV Model	30
3.3 PV Model	33
3.4 Grid Model	34
4 MPC-BASED CENTRALISED POWER CONTROL DESIGN	37
4.1 Modelling Methodology	38
4.1.1 Arrivals model	39
4.1.2 PV Adaptation Method	43
4.2 Optimization Problem Methodology	43
5 IMPLEMENTATION AND SIMULATION SETUP	49
5.1 EV Parameters	50
5.2 Battery Parameters	51
5.3 Grid Parameters	51
5.4 PV Parameters	52

6	RESULTS AND ANALYSIS	55
6.1	Grid Power Performance	55
6.2	Battery Power Performance	56
6.3	Performance on EV Charging Coordination	58
6.4	Performance Comparison on Power Allocation	60
6.5	Time Complexity to Solve OP	61
7	CONCLUSION	63
	REFERENCES	65

Listing of figures

2.1	Interactions between EVs and the smart grid[1].	6
2.2	Charging at (a) variable rates and (b-c) discrete rates [1].	6
2.3	Total number of publicly accessible charging points, according to the AFIR categorization: (a) AC charging and DC charging; (b) Pie plot of the CP share in EU @2022.	8
2.4	Centralized EV charging control architecture and variations of distributed (decentralized, hierarchical) EV charging control architectures [1].	8
2.5	Control scheme architecture of MPC.	10
2.6	Proposed two-stage energy management scheme for the charging station [2]	12
4.1	Probability distribution function of Poisson distribution.	40
4.2	Probability distribution function of uniform distribution.	42
5.1	The expected PV Power production for a sunny day	52
5.2	The Real PV Power Production for a cloudy day	53
6.1	The expected power of the grid vs its real power during the day	55
6.2	The expected power of the battery vs its real power during the day	56
6.3	The SOC of the ESS battery	57
6.4	The EVs charging rate in period out of peak hours	58
6.5	The EVs charging rate in the period of peak hours	59
6.6	The SOC of EVs in the period out of peak hours	59
6.7	The SOC of EVs in the period of peak hours	60
6.8	The total power flow exchanged through the network	61
6.9	The time complexity to solve the optimization problem with respect to the horizon time	62

Listing of tables

5.1	Rate of the EVs arrival with the Poisson distribution model	50
5.2	EVs battery parameters and constraints	50
5.3	ESS battery parameters and its constraints	51

Listing of acronyms

ICE	Internal Combustion Engine
PV	Photovoltaic
EMS	Energy Management System
EV	Electric Vehicle
V₂G	Vehicle to grid
RES	Renewable Energy Source
ESS	Energy storage System
CP	Charging Point
DC	Direct current
AC	Alternating Current
DR	Demand Response
MPC	Model Predictive Control
DSM	Demand Side Management
E_{req}	Energy Required
t_{arr}	Time of arrival
t_{dep}	Time Of Departure
Flx	Flexibility Of Required Energy
SOC	State Of Charge
OP	Optimization Problem
NE	Nash Equilibrium
BR	Best Response

GNE Generalized Nash Equilibrium
KKT Karush-Kuhn-Tucker
 E_{req} Energy required [E_{init}]*Initial stored energy*

1

Introduction

The target of the 2030 UN's Agenda for Sustainable Development related to ensuring access to affordable, sustainable, and modern energy are aligned with the global effort to address climate change, promote clean energy, and achieve sustainable development[3]. These targets are outlined in sustainable Development goal and focus on ensuring access to reliable and sustainable energy. Indeed, smart grids play a crucial role in enhancing the efficiency of electricity utilization throughout the entire electricity supply chain, from generation to end-users, it enables real-time monitoring of electricity generation, transmission, and consumption. Smart grids provide the infrastructure and technologies to integrate renewable energy sources (RESs), such as solar and wind power, into the grid. These sources are intermittent and vary with weather conditions, but smart grids can forecast their output and coordinate their integration with conventional generation to ensure a stable and efficient power supply. It allows also for the integration of energy storage systems (ESS), such as batteries, pumped hydro, and flywheels. These storage solutions help capturing excess of electricity during periods of low demand or high renewable energy generation and release it during peak demand periods. Electric vehicles (EV) have gained immense popularity due to their environmental benefits and reduced dependency on fossil fuels [4][5]. They are powered by electric motors and use rechargeable batteries to store energy. EVs can be charged using various methods, including standard AC charging from the power grid or fast DC charging stations[6]. On the other hand, concerns have been raised about the peak power requirements for recharging EV batteries. Some people are worried that the existing electrical infrastructure might not be able to handle the simultaneous demand

electricity during peak charging periods[7]. Demand response (DR) was already recognised as a crucial mechanism in the coordination of energy production and consumption, especially with the increasing adoption of renewable energy sources and the growth of prosumers [8]. In the context of prosumers, demand response becomes even more significant. Prosumers can generate excess of electricity when their renewable energy sources produce more than their own consumption needs. Instead of wasting this surplus energy or feeding it back into the grid at times when it might not be needed, demand response mechanisms allow prosumers to respond to market signals and adjust their consumption or sell the excess of energy to the grid when electricity prices are high[9]. An efficient management system for prosumers requires the development and implementation of advanced control strategies that enhance demand flexibility and minimize economic expenditures[10]. In this context, model predictive control (MPC) is being considered as a promising control strategy for efficiently managing users resources. MPC is a control methodology used in engineering and industrial processes to optimize the control of a system. It is particularly well-suited for systems with constraints and dynamic behaviour, making it an effective approach for managing resources in various applications[11][12].

In this work, the model predictive control is used to manage a station that contains a certain number of EV chargers with a PV source, an energy storage system and a connection to the upstream grid. Predictive control can be employed to efficiently manage these resources while recharging the battery of an EV and respecting operational constraints. The primary objective of this control is to maximize the utilization of renewable energy from the PV source and ESS while ensuring that the EV battery is adequately charged. A typical scenario assumes that the EVs battery is recharged during the day to take advantage and into consideration PV production. The available energy resources are effectively managed by predictive control system. The focus of this study is on a centralised control approach, where the power distribution system is centrally managed, and power dispatch decisions are made based on model predictive control. The study revolves around power distribution systems, which involve the distribution of electrical power from the grid to various end-users, including EV and PV. This study employs MPC as the primary control algorithm, which is known for its ability to predict future system behaviour and optimize control actions accordingly. It also involves demand-side management (DSM) techniques, allowing for load shifting and peak shaving to reduce overall system costs and improve grid stability. In the real world implementation of a centralized MPC-based control system in a power distribution network may face practical challenges like data availability, communication delays, and hardware constraints. MPC algorithms can be computationally intensive, particularly when dealing with large-scale power distribution systems with numer-

ous EVs and PV systems. The study may not fully capture the human behavioral aspects of EV owners, which can influence charging patterns and may not always align with MPC optimization objectives.

The organization of the thesis is as follows. In section 2, we give a comprehensive review, presenting an overview of existing research on power distribution systems, EV integration, and PV coordination, laying the foundation for the proposed MPC-based control strategy. Section 3, we focus on detailing the system model and assumptions, providing a clear understanding of the power distribution system and the parameters considered in the MPC formulation. Section 4, we describe the proposed energy management system based on MPC. Section 5, outlines the simulation setup, specifying the environment and parameters employed in the experiments. In section 6, MPC-based control is evaluated and compared with conventional (heuristic) control. The conclusion is reported in section 7.

2

Literature And Review

2.1 OVERVIEW OF POWER DISTRIBUTION SYSTEM

A power distribution system is an essential part of the electricity grid that plays a vital role in delivering electricity from the higher voltage transmission system to end-users, such as residential, commercial, and industrial consumers[13]. It forms the final link in the chain of power delivery, ensuring that electricity reaches consumers reliably and efficiently.

2.2 EV AND PV INTEGRATION IN POWER DISTRIBUTION SYSTEM

Electric vehicle integration in the power distribution system is significant and evolving challenge for power utilities and grid operators as electric transportation becomes more prevalent. The integration of EVs introduces both opportunities and challenges in the power distribution system[14]. EVs can act as distributed energy resources, providing flexibility to the grid. Through vehicle-to-grid (V2G) technology[15], EVs can discharge stored electricity back to the grid during peak demand periods, helping to balance loads and support grid stability. Smart charging and demand response strategies can be employed to manage EV charging optimizing the timing and rate of charging to avoid overloading the grid during peak hours. Also EVs can be utilized to provide ancillary services to the grid, such as frequency regulation and voltage

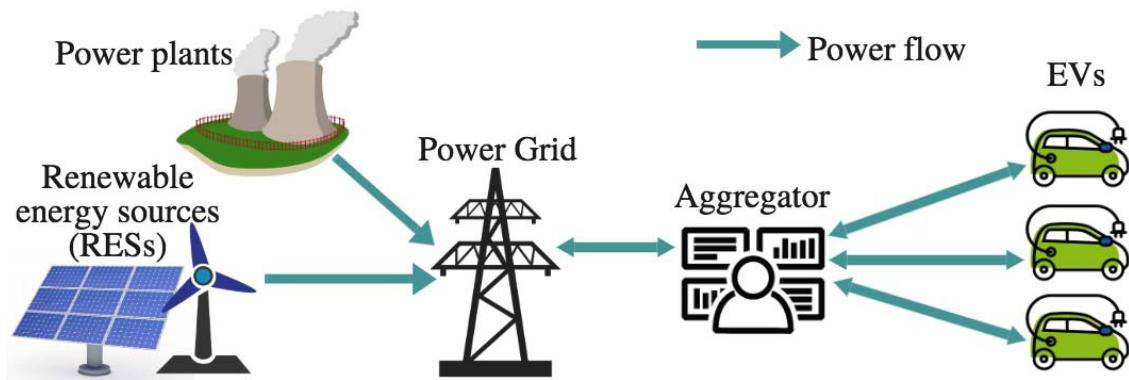


Figure 2.1: Interactions between EVs and the smart grid[1].

support, contributing to grid reliability. In the other side, high concentration of EVs charging simultaneously in specific areas can lead to grid congestion and require grid upgrades to accommodate the increased demand. In figure 2.1, the aggregator acts as a central entity that communicates with a large numbers of EVs. Instead of individual EVs interacting directly with the grid operator or electricity market, they interact with the aggregator.

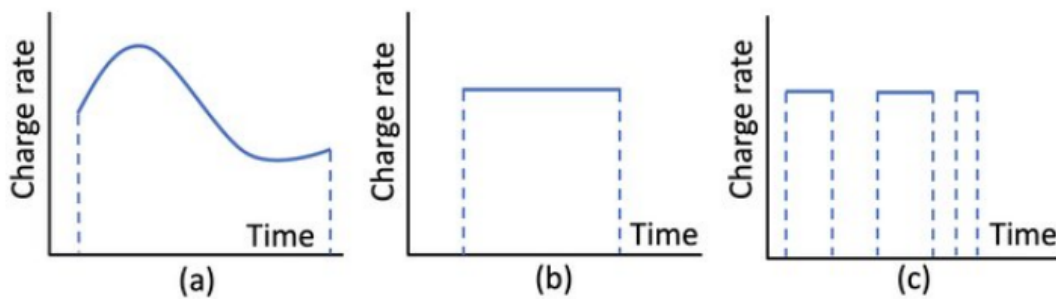


Figure 2.2: Charging at (a) variable rates and (b-c) discrete rates [1].

Another important parameter is the charging rate. In the literature, the electric vehicle charge rate is often treated as a continuous variable that can take any value within specific range[16]. Continuous variable provides flexibility in modelling charging scenarios and in optimization problems. They enable the use of mathematical techniques, such as calculus and optimization algorithm, to find optimal charging strategies and grid management solutions. However, it is important to note that in practical implementations, the charge rate is often discredited due to technical limitations that impose to align with a specific charging levels (e.g.,

level 1, level 2, level 3 charging) as shown in figure 2.2 . Moreover discrete-rate chargers with on-off controllers have simpler design, requiring fewer components and less complex circuitry. This simplicity reduces manufacturing costs and makes them more affordable for consumers and charging infrastructure providers. One of the advantages of employing discrete charging, where the charger operates with on-off cycles during idle slots, is that it allows the EV battery to cool down between charging sessions. This cooling effect can positively impact the battery's overall health and extend its life[17]. Another parameter that can make power distribution system more complex is homogeneous or heterogeneous EV specification. While some EV charge scheduling algorithms may perform well for an homogeneous or identical EV population[18], practical algorithms must be able to handle the challenges posed by an heterogeneous EV population. Heterogeneous in various charging specifications and user preferences is common in real-world scenarios, and an effective algorithm should be capable of accommodating these variations. The EU Alternative Fuels Infrastructure Regulation (AFIR) defines two categories of charging points for electric vehicles based on the topology of connection between the vehicle and the charging station:

- Category 1: Charging points (CPs) that provide an alternate current (AC) output power, and the battery charging is managed by the electric vehicle's on-board charger. In this mode, the AC power is supplied to the vehicle, and the vehicle's on-board charger is responsible for converting this AC power to direct current (DC) to charge the vehicle's battery.
- Category 2: CP that provides a DC output power, and the battery charging is managed directly by the off-board converter installed inside the charging station. In this mode, the charging station supplies DC power directly to the vehicle's battery, by passing the need for the vehicle's on-board charger to convert AC to DC. The majority CPs in the EU, accounting for 88 %, fall under the AC category, According to the pie plot in figure 2.3b, approximately 73 % of these AC CPs offer power outputs ranging from 7.4 KW to 22 KW, while around 11 % have a power rating below 7.7 KW.

In contrast, the DC charging category constitutes only 11 % of the total CPs. Among the DC CPs, the highest proportion, 5.5 % provides power ratings between 50 KW and 150 KW, making them the most common within the DC charging category. Additionally, a smaller portion of DC CPs, around 3.8 % offers ultra-fast charging, also known as level 1.

PV integration can occur at various scales, including residential, commercial, and utility-scale installations[19]. Solar panels are installed at suitable locations such as rooftops, open

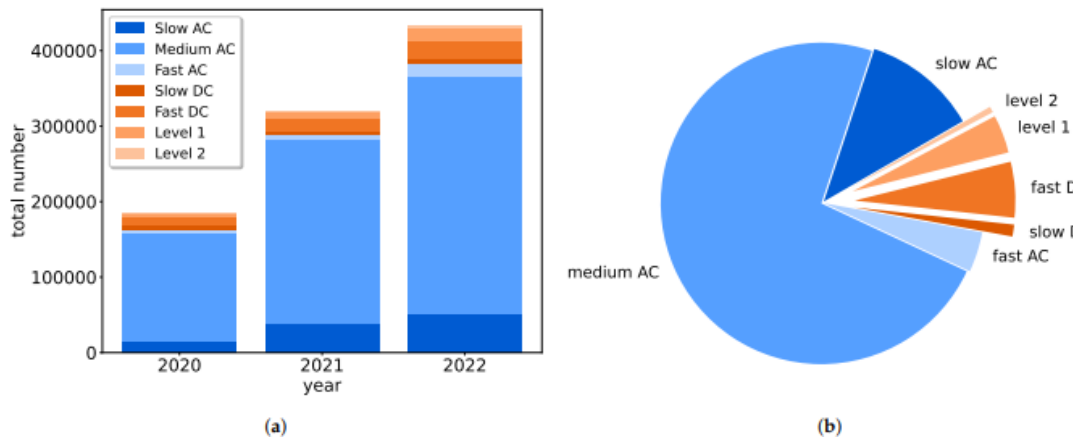


Figure 2.3: Total number of publicly accessible charging points, according to the AFIR categorization: (a) AC charging and DC charging; (b) Pie plot of the CP share in EU @2022.

fields, or solar farms. These panels consist of multiple solar cells that convert sunlight into DC electricity. PV integration enables distributed generation, where electricity is produced close to the point of consumption. This can reduce transmission losses and ease stress on the transmission infrastructure, it produces electricity during peak demand hours, which can help offset the higher energy demand during those times and potentially reduce the need for additional peaking power plants.

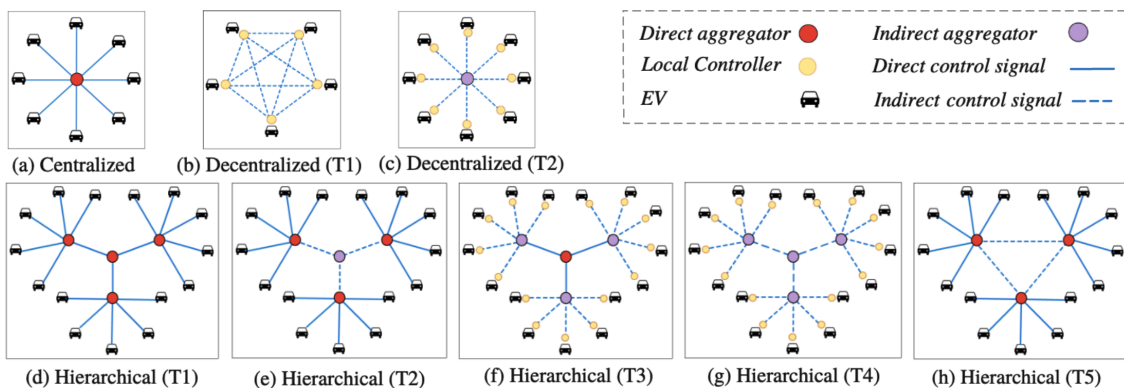


Figure 2.4: Centralized EV charging control architecture and variations of distributed (decentralized, hierarchical) EV charging control architectures [1].

2.3 CENTRALISED POWER CONTROL AND MPC IN POWER SYSTEM

Centralized power control refers to a system in which the authority and decision-making capabilities are concentrated in a single entity or a small group of individuals[20]. In the context of EVs, as shown in figure 2.4a central entity collects and processes the charging requirements of all the connected EVs. Its main function is to coordinate and optimize the charging schedules of these EVs based on various factors such as grid demand, electricity prices, and individual vehicle needs. By allowing the aggregator to coordinate and control EV charging schedules, EV owners become part of a collective effort to optimize electricity usage and promote sustainable energy practices. EV owners relinquish some autonomy over their charge schedule to the centralized aggregator. This is a necessary trade-off to achieve the benefits of optimized charging and grid management. The level of autonomy relinquished can vary based on the specific implementation of the aggregation system and the preferences of the EV owners. Some key aspects of autonomy relinquished may include charging time, charging rate and energy required. The challenge arises from the fact that as the number of connected EVs and the planning time horizon increase, the size and complexity of the optimization problem (OP) grow exponentially. This complexity requires significant computational resources and time to find optimal or near-optimal solutions. As a result, the centralized approach may struggle to handle the increasing workload, potentially leading to slower response times, inefficient scheduling, and overall reduced system performance.

Model predictive control (MPC) is control strategy commonly used in power systems to optimize the operation of power plants, energy storage systems, and other devices to achieve desired performance objectives[21]. However, MPC implementation in power systems requires accurate models, real-time data, and significant computational resources as shown in fig . The quality of model and accuracy of predictions are critical for the success of the control strategy. Therefore, the development of accurate models and access to real-time data are essential considerations when applying MPC in power systems.

2.4 PREVIOUS STUDIES

There are various works and research papers focused on EV charging techniques[22]. In reference [23], a strategy was formulated for power dispatch and charging at a battery swap sta-

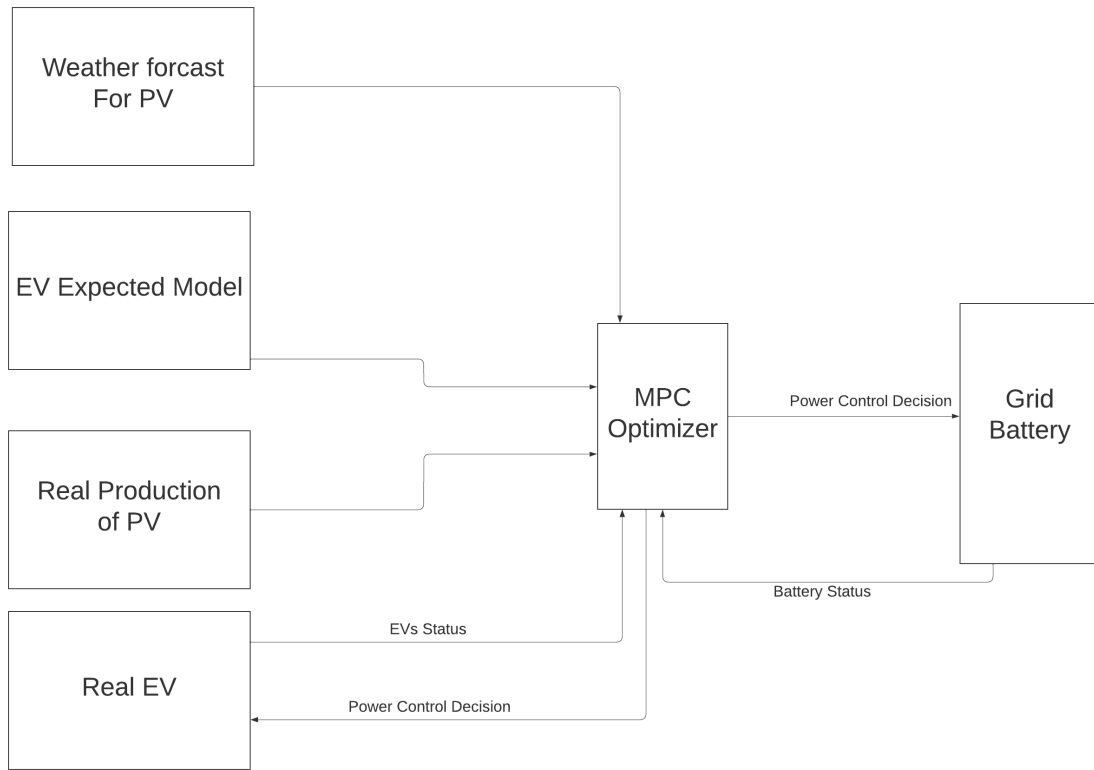


Figure 2.5: Control scheme architecture of MPC.

tion using PV energy. The strategy takes into account both the efficient utilization of PV energy and the availability of swapping services. In [24], an outlined strategy aimed at improving the charging station operational cost efficiency, making use of PV and battery energy sources, was centered around the implementation of the chance-constrained optimization. A charging mechanism involved in [25], using predicted PV generation power and EV arrival/departure times to determine the energy generation and EV charging strategy. In [26], a day-ahead scheduling framework was examined, with the goal of optimizing the operational scheduling for both a micro grid and an EV battery swapping station. [27] presented a distributed-control-based scheduling system for EV charging. Nevertheless, this approach did not incorporate PV and battery, primarily concentrating on leveraging the charging flexibility of EVs while overlooking their diverse charging requirements. Game-theory-based approaches have gained significant popularity in addressing the control problem of energy management [28], as they effectively capture the individual characteristics and decentralized nature of the system. In the existing schemes discussed in [29] and [30], the order of energy utilization prioritized renew-

able sources, followed by battery storage, and finally, the grid. This sequential approach aimed to minimize grid energy consumption. Nevertheless, this sequential approach may lead to the rapid depletion of the battery's energy, ultimately forcing the grid to shoulder the entire load. As a result, the intended purpose of using the battery is to alleviate the grid's burden when it cannot be fully realized due to its limited utilization. Among previous studies we choose another related paper and study it in details.

Paper study

The title of this paper is: A Two-Stage Scheme for Both Power Allocation and EV Charging Coordination in a Grid-Tied PV-Battery charging station [2]. The primary contributions of this article can be succinctly summarized in the following manner:

- Introduction of two-stage methodology that effectively addresses two key challenges: the allocation of power among PV, battery, and the grid, as well as the coordination of EV charging in situations of insufficient and fluctuating power availability
- Expansion of the application of a game theory to encompass not just dispatching EV charging, but also power allocation across PV, battery and grid resources.
- Direct determination of the total EV charging power, accounting for physical limitations.
- Examination of the two-stage strategy in both grid-tied and islanded operational modes.

Problem Formulation

The EV charging station under study is equipped with both PV and a battery connected to the grid. The station experiences random and dynamic arrival of EV seeking to charge. The charging station supplies the overall charging power needed by the EVs. This total charging power is derived from a combination of PV-generated electricity, battery storage, and power from the grid. The process of determining the specific portion of power provided by each of these sources holds significant importance. Notably, due to the station's limited power capacity, it may not always be able to fulfill the charging requirements of all EVs. This particular aspect diverges from conventional scenario, where the goal is to match supplied power with demand. In this paper the problem is divided into two stage as shown in figure 2.5 , the first stage is about the power allocation among power resources depending on the power demand. The second stage is about dispatching the available power through the existing EVs.

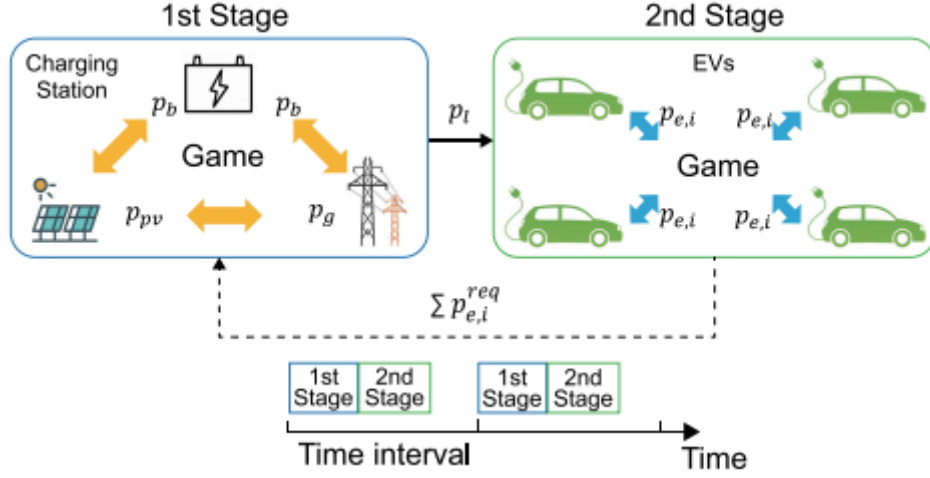


Figure 2.6: Proposed two-stage energy management scheme for the charging station [2]

A) The first stage

The issue of distributing power is mathematically presented as a non cooperative game. The PV, battery, and the grid are considered as separate entities, akin to three distinct players. In this game scenario, these players are assumed to act with self-interest, striving to maximize their individual utilities.

Battery Utility Function

In this paper, it is important to uphold a specific and preferred SOC of the battery. This enables the battery to swiftly discharge or store the power, thereby establishing an ample regulatory buffer for potential rapid adaptation. The utility function u_b for the battery is defined as follows:

$$u_b(t) = -\frac{1}{2}(p_b(t) - p_{bf}(t))^2 \quad (2.1)$$

where $p_b(t)$, and $p_{bf}(t)$ are the power flow of the battery and preferred power of the battery respectively. p_{bf} is directly related to the SOC of the battery as follows:

$$p_{bf}(t) = \left(\frac{SOC_b(t) - SOC_{bf}}{SOC_{b,max} - SOC_{b,min}} \right) p_{b,max} \quad (2.2)$$

Where SOC_{bf} is the preferred state of charge, $[SOC_{b,min} \quad SOC_{b,max}]$ and $[p_{b,min} \quad p_{b,max}]$ are the battery permitted SOC and the power operation range, respectively. The minimum SOC and maximum SOC are employed to protect the battery from degradation. When $SOC(t)$ of the battery is less than the preferred SOC_{bf} , the preferred power of the battery will be negative,

which means the battery tends to charge. When the $SOC(t)$ is greater than the preferred SOC_{bf} , the preferred power will be positive, which means that the battery tends to discharge and gives power to the network. The operational constraint of the battery are as follows:

$$SOC_{b,min} \leq SOC_b(t) \leq SOC_{b,max} \quad (2.3)$$

$$p_{b,min} \leq p_b(t) \leq p_{b,max} \quad (2.4)$$

The dynamic of the battery is as follows:

$$SOC_b(t+1) = \begin{cases} SOC_b(t) - p_b(t)\Delta t/E_b/\eta_d; & \text{if } p_b(t) > 0 \\ SOC_b(t) - p_b(t)\Delta t\eta_c/E_b; & \text{if } p_b(t) \leq 0 \end{cases} \quad (2.5)$$

$$SOC_b(0) = SOC_{b,init} \quad (2.6)$$

where E_b , η_d , η_c and $SOC_{b,init}$ are the battery normal energy, battery discharge efficiency, and initial SOC value respectively. From the dynamics of the battery, the power given by the battery to the network will be reduced by certain amount depending on the efficiency, also the power given by the network to the battery will be reduced depending on the charging efficiency. $p_b(t)$ is a continuous signal that can take any value between the maximum and the minimum boundaries. This would help to manage the energy through the network.

PV Model

Typically, solar photovoltaic (PV) panels are presumed to operate in a mode where they actively seek the maximum power point of their output. An approximate value for this power referred to as p_{mp} can roughly calculated as:

$$p_{mp}(t) = G_i(t)A_{pv}\eta_{pv} \quad (2.7)$$

where G_i is the solar irradiance, A_{pv} is the installed PV panels surface area, and η_{pv} is the conversion efficiency.

While the PV generation undoubtedly has the potential to decrease the energy drawn from the conventional power grid, the swift and the unpredictable variations in solar power output can lead to an unanticipated breaches in voltage thresholds. Hence, it becomes imperative to enforce the limitations on the rate at which PV power can change, denoted as $p_{pv,rp}$, in the follow-

ing manner:

$$p_p(t) - p_p(t-1) \leq p_{pv,rp} \quad (2.8)$$

where $p_p(t)$ is the PV power production at time t . It is worth acknowledging that adhering to this power ramping restriction unavoidably brings a reduction in the PV generation due to the relinquished opportunity for utilizing the untapped energy. Hence, the utility function governing the performance of the PV system is designed with a primary focus on delivering the power that closely aligns with the optimal point, which leads to the least curtailment-related losses. In this context, the utility function, denoted as u_p , is formulated as follows:

$$u_p(t) = -\frac{1}{2}(p_p(t) - p_{mp}(t))^2 \quad (2.9)$$

From this definition we see that the utility will decrease when the power of PV is different from the maximum power, but this latter will not affect other utility functions. So instead of adding this utility function, we could only impose a constraint, such that the power of PV will be as follows:

$$p_p(t) = \min(p_{t-1} + p_{pv,rp}, p_{mp}(t)) \quad (2.10)$$

$$p_p(t) \leq p_{mp} \quad (2.11)$$

Grid Model

The utility function of the grid, denoted as u_g , is designed to prioritize the economy by focusing in reducing the electricity consumption from the grid. Just like the utility functions of the battery and the PV systems, the grid utility function can be expressed as follows:

$$u_g(t) = -\frac{1}{2}(p_g(t) - p_{g,opt})^2 \quad (2.12)$$

Under the constraints:

$$0 \leq p_g(t) \leq p_{g,max} \quad (2.13)$$

$$|p_g(t) - p_g(t-1)| \leq p_{g,rp} \quad (2.14)$$

Here, $p_{g,opt}$ represents the preferred power output of the grid, which in this case is set to zero to indicate no energy consumption from the grid. This function indicates that the utility function u_g is maximized when there is no power output from the grid. Conversely, a significant amount

of the power output is considered unfavorable. It is important for the grid's power output to adhere to both power capacity limits $[0, p_{g,max}]$, and ramping power limits. In this case the power limits ramping is considered in both way either when the power is reduced or when it is increased, unlike the PV power ramping.

Modified utility function

The desired charging power for EVs, denoted as $p_{e,i}^{req}$ represents the charging power that the i th EV requests from the charging station. Let I be the set of EVs currently connected for charging. We define p_l^* as the sum of all individual desired charging power requirements.

$$p_l^* = \sum_{i \in I} p_{e,i}^{req} \quad (2.15)$$

And $p_l(t)$ represents the actual total charging power supplied by the combination of the PV, the battery, and the grid sources, specifically:

$$p_l(t) = p_g(t) + p_p(t) + p_b(t). \quad (2.16)$$

Furthermore, a constraints exists to keep the power balance in the network:

$$p_l(t) \leq p_l^* \quad (2.17)$$

In light of these considerations, the objective of the charging station is to maximize the following utility function:

$$u_l(t) = -\frac{1}{2}(p_l(t) - p_l^*)^2 = -\frac{1}{2}(p_g(t) + p_p(t) + p_b(t) - p_l^*)^2 \quad (2.18)$$

As observed, the utility function $u_l(t)$ reaches its maximum value precisely when the supplied power aligns perfectly with the EV's required power. Additionally, the actions taken by each participant also influence $u_l(t)$. Thus, a potential resolution involves the integration of the $u_l(t)$ utility function with those of other participants. Consequently, the ultimate configuration of each player's utility function is adjusted as follows:

$$u_{p,l}(t) = u_p(t) + w_{l,p}u_l(t) \quad (2.19)$$

$$u_{b,l} = u_b + w_{l,b}u_l \quad (2.20)$$

$$u_{g,l} = u_g + w_{l,g}u_l \quad (2.21)$$

where $w_{l,p}$, $w_{l,g}$, and $w_{l,b}$ are a positive weights. Consequently, the final term in each adjusted utility function works as a penalty component. This gives rise to the logical interpretation that each energy source (PV, battery, and the grid) strives to optimize its individual utility. Simultaneously, these sources are obliged to contribute to minimize the curtailment of overall charging demand to the greatest extent possible.

Noncooperative Game

This article describes a noncooperative game scenario involving a three players: the photovoltaic system (PV) represented by P , the grid represented by G , and the battery represented by B . Each player is attempting to maximize its own utility function. The utility function's value for each player depends not only on its own control variable but also on the decisions made by the other players and the required charging power of the EVs.

In this setup, the players are considered selfish, meaning that they aim to optimize their own outcomes without necessarily coordinating with the others. This kind of game is analysed using the concept of Nash equilibrium (NE), which is a situation in which no player can unilaterally change their decision to improve their own outcome, given the decisions of the other players. The utility functions mentioned are concave for each player, which helps ensure the existence and the uniqueness of the Nash equilibrium. Concavity is a property that ensures that if a player try to deviate from the current equilibrium, it will not be able to achieve a better outcome without affecting the other player's utility.

The Nash equilibrium can be found by solving the best response (BR) functions. A best response is the optimal strategy for a player given the strategies chosen by the other players. Solving the BR functions involves finding the strategies that maximize each player's utility, taking into account the decisions of the other players and the constraints of the game.

$$BR_p : \frac{\partial u_{p,l}}{\partial p_p} = 0, \quad BR_g : \frac{\partial u_{g,l}}{\partial p_g} = 0, \quad BR_b : \frac{\partial u_{b,l}}{\partial p_b} = 0. \quad (2.22)$$

Then we can obtain:

$$\begin{aligned}
BR_p : p_p^+ &= \frac{p_{mp} - w_{l,p}(p_g + p_b - p_i^*)}{1 + w_{l,p}} \\
BR_g : p_g^+ &= \frac{-w_{l,g}(p_b + p_p - p_i^*)}{1 + w_{l,g}} \\
BR_b : p_b^+ &= \frac{p_{bf} - w_{l,b}(p_g + p_p - p_i^*)}{1 + w_{l,b}}
\end{aligned} \tag{2.23}$$

$$\begin{aligned}
H_{p,l} : -(1 + w_{l,p}) &< 0 \\
H_{g,l} : -(1 + w_{l,g}) &< 0 \\
H_{b,l} : -(1 + w_{l,b}) &< 0
\end{aligned} \tag{2.24}$$

As described in the paper, the Hessian for the utility functions of each player is negative definite. However, the Hessian of the utility function should be a matrix of (3×3) second-order partial derivatives that provides an information about the curvature of a function at a specific point. In order to calculate the Hessian we have first to calculate the Gradient of each utility function. The gradient of $U_{p,l}$ is:

$$\nabla U_{p,l} = \begin{bmatrix} \frac{\partial u_{p,l}}{\partial p_p} \\ \frac{\partial u_{p,l}}{\partial p_g} \\ \frac{\partial u_{p,l}}{\partial p_b} \end{bmatrix} = \begin{bmatrix} -(p_p - p_{mp}) - w_p(p_p + p_g + p_b - p_i^*) \\ -w_p(p_p + p_g + p_b - p_i^*) \\ -w_p(p_p + p_g + p_b - p_i^*) \end{bmatrix} \tag{2.25}$$

The Hessian H_p of $U_{p,l}$ function is:

$$H_p = \begin{bmatrix} \frac{\partial^2 u_{p,l}}{\partial p_p^2} & \frac{\partial^2 u_{p,l}}{\partial p_p \partial p_g} & \frac{\partial^2 u_{p,l}}{\partial p_p \partial p_b} \\ \frac{\partial^2 u_{p,l}}{\partial p_g \partial p_p} & \frac{\partial^2 u_{p,l}}{\partial p_g^2} & \frac{\partial^2 u_{p,l}}{\partial p_g \partial p_b} \\ \frac{\partial^2 u_{p,l}}{\partial p_b \partial p_p} & \frac{\partial^2 u_{p,l}}{\partial p_b \partial p_g} & \frac{\partial^2 u_{p,l}}{\partial p_b^2} \end{bmatrix} = \begin{bmatrix} -1 - w_p & -w_p & -w_p \\ -w_p & -w_p & -w_p \\ -w_p & -w_p & -w_p \end{bmatrix} \tag{2.26}$$

The Hessian matrix is symmetric $H_p^T = H_p$, the spectrum of the Hessian are as follows:

$$Spec(H_p) = \left\{ \lambda_1 = 0, \quad \lambda_2 = \frac{-3w_p - \sqrt{9w_p^2 - 8wp}}{2}, \quad \lambda_3 = \frac{-3w_p + \sqrt{9w_p^2 - 8wp}}{2} \right\} \tag{2.27}$$

From (2.27), the Hessian of the utility function $U_{p,l}$ is negative semi-definite. In similar way:

$$H_g = \begin{bmatrix} -w_g & -w_g & -w_g \\ -w_g & -1 - w_g & -w_g \\ -w_g & -w_g & -w_g \end{bmatrix} \quad (2.28)$$

$$H_b = \begin{bmatrix} -w_b & -w_b & -w_b \\ -w_b & -w_b & -w_b \\ -w_b & -w_b & -1 - w_b \end{bmatrix} \quad (2.29)$$

The Hessian of H_g and H_p are negative semi-definite. The negative semi-definiteness of the hessian of the best response utility function indicates that the utility function is concave in the vicinity of the best response. This is important because it implies that the best response strategy is a maximizer. an equilibrium where each player strategy is a best response to the others strategies is often of interest. If the hessian of each player best response strategy is negative semi-definite, it contributes to the stability of the equilibrium point, avoiding the other players from deviating from their strategies.

Overall, the scenario described involves a game theoretic approach to modelling the interactions and decision-making of a selfish players in a noncooperative environment, aiming to find a point of equilibrium where no player has an incentive to unilaterally deviate from their current strategy.

Let $P = [p_p \ p_g \ p_b]^T$. The solution of the best response can be described as linear dynamical system:

$$P^+ = F(P) = AP + \bar{P} \quad (2.30)$$

$$A = -diag(W) \begin{pmatrix} 0 & 1 & 1 \\ 1 & 0 & 1 \\ 1 & 1 & 0 \end{pmatrix} \quad (2.31)$$

where

- $W = [W_1 \ W_2 \ W_3]$
- $W_1 = \frac{w_{l,p}}{1+w_{l,p}}$
- $W_2 = \frac{w_{l,g}}{1+w_{l,g}}$
- $W_3 = \frac{w_{l,b}}{1+w_{l,b}}$

$$\bullet \bar{P} = \begin{bmatrix} \frac{p_{mp} + w_{l,p} p_l^*}{1 + w_{l,p}} & \frac{w_{l,g} p_l^*}{1 + w_{l,g}} & \frac{p_{bl} + w_{l,b} p_l^*}{1 + w_{l,b}} \end{bmatrix} T$$

The equilibrium point can be obtained as follows:

$$P_{eq} = AP_{eq} + \bar{P} \rightarrow P_{eq} = (I - A)^{-1} \bar{P} \quad (2.32)$$

Let $\tilde{P} = P - P_{eq}$ be the deviation from the equilibrium point. Then the dynamic of \tilde{P} can be expressed as follows:

$$\tilde{P}^+ = A\tilde{P} \quad (2.33)$$

To have a stable equilibrium point, A should be Schur stable. A matrix is Schur stable if all of its eigenvalues lie within the open unit disc of the complex plane. In other words, the absolute value of each eigenvalue is less than 1.

Using GERSHGORIN theorem, the eigen value of the matrix A will be inside the circles of center 0 and radius $\frac{2w_p}{1+w_p}$, $\frac{2w_g}{1+w_g}$ and $\frac{2w_b}{1+w_b}$. Hence, we have stability if $0 < w_p < 1$, $0 < w_g < 1$ and $0 < w_b < 1$.

Algorithm 2.1 Power Allocation for Charging Station.

- 1: **initialization** $p_{p,last} \leftarrow p_{p,t-1}, p_{g,last} \leftarrow p_{g,t-1}, p_{b,last} \leftarrow p_{b,t-1}$.
 - 2: **repeat**
 - 3: solve p_g^+ via BR_g using $p_{b,last}$ and $p_{p,last}$ and check (2.13) and (2.14)
 - 4: solve p_p^+ via BR_p using $p_{g,last}$ and $p_{b,last}$ and check (2.8) and (2.10)
 - 5: solve p_b^+ via BR_b using $p_{g,last}$ and $p_{p,last}$ and check (2.3) and (2.4).
 - 6: **check convergence:**
 - 7: **if** $|p_p^+ - p_{p,last}| \leq \varepsilon$ **and** **if** $|p_g^+ - p_{g,last}| \leq \varepsilon$ **and** **if** $|p_b^+ - p_{b,last}| \leq \varepsilon$.
 - 8: terminate
 - 9: **else**
 - 10: $p_{p,last} \leftarrow p_p, p_{g,last} \leftarrow p_g, p_{b,last} \leftarrow p_b$
 - 11: **end if**
 - 12: **Until** convergence
 - 13: solve p_l via (14) and send p_l to the second stage.
-

Algorithm 2.1 outlines a procedure for iteratively updating the decisions of the PV, the grid, and the battery players based on their respective best response functions. The algorithm aims to find a Nash equilibrium where the players decisions are balanced, while also calculating the total available charging power for EVs. The design of the algorithm takes into account the privacy considerations to preserve the local information of the players. Here's a breakdown of the algorithm's steps:

- 1. **Initialization:** The algorithm starts by initializing the players' decisions from the previous time instant $p_{p,t-1}$, $p_{g,t-1}$, and $p_{b,t-1}$.
- 2. **Grid Decision Update:** The grid player aims to maximize its utility function $u_{g,l}$. It calculates its new decision p_g^+ using BR_g function while keeping the decisions of the other players constant ($p_p=p_{p,t-1}$ and $p_b=p_{b,t-1}$). The updated grid decision is stored as $p_{g,t-1}$.
- 3. **PV and Battery Decisions updates:** Similarly, the algorithm updates the decision of the PV and the battery players using their respective best response functions BR_p and BR_b . These updates are stored as $p_{p,t-1}$ and $p_{b,t-1}$.
- 4. **Iterative Convergence:** The algorithm iteratively repeats steps 2 and 3 until the decisions p_p , p_b and p_g converge to a stable point. This convergence signifies that the Nash equilibrium of the game has been reached.
- 5. **Total Available Charging Power calculation:** Once the decision have converged, the total available charging power p_l can be calculated .
- 6. **EV charging Coordination:** The players only share their control variables ($p_p(t)$, $p_b(t)$ and $p_g(t)$) and the total required charging command p_l^* with the EV charging side. This design preserves the players local privacy information.

Lines (3, 4, 5) suggest the solutions for p_g^+ , p_p^+ , p_b^+ with the assumption that the operational constraints will be satisfied, but in case the operational constraints are not satisfied, algorithm (2.1) does not propose an alternatives. One other approach to solve this problem, we use the following:

$$\begin{aligned}
 p_g^+ &= \underset{p_g}{\operatorname{argmax}} U_{g,l}(p_g, p_b, p_p), \text{ subjected to (2.13)} \quad (2.14) \\
 p_b^+ &= \underset{p_b}{\operatorname{argmax}} U_{b,l}(p_g, p_b, p_p), \text{ subjected to (2.3)} \quad (2.14) \quad (2.5). \quad (2.34) \\
 p_p^+ &= \underset{p_p}{\operatorname{argmax}} U_{p,l}(p_g, p_b, p_p), \text{ subjected to (2.8)} \quad (2.10)
 \end{aligned}$$

B) The second Stage

In the second stage of the charging coordination process, the EVs determine their shared portion of the total charging power p_l based on their individual preferences and requirements. Here's a breakdown of the concepts:

- **EV charging coordination:** In the second stage of the charging process, individual EVs need to allocate their portion of the total charging power p_l determined in the first stage.

This stage is often referred to as EV charging coordination, and its goal is to efficiently allocate the available charging resources among the EVs.

- **Consideration of Diversities:** EVs have diverse characteristics including different charging power requirements, charging preferences, and urgency levels. Some EVs might need quick charging even if it means paying a higher electricity price, while others might be more flexible in their charging needs. The coordination process needs to take these diversities into account to ensure fair and efficient resource allocation.
- **Flexibility and Game Theory:** Game theory is applied to address the EV charging coordination problem due to its distributed nature and ability to respect the preferences of individual EVs. In this context, each EV is treated as an independent player in a noncooperative game. The use of the game theory allows the EVs to make strategic decisions based on their preferences and requirements while competing for the available total charging power.
- **Noncooperative Game Model:** The EV charging coordination problem is modeled as a noncooperative game, where each EV is a player seeking to maximize its own utility or satisfaction. The EVs independently decide how much of the total charging power p_l to allocate to themselves, taking into consideration factors such as their charging requirements, urgency, and willingness to pay for faster charging.
- **Competition and Allocation:** In this game, the EVs compete for the shared charging resource p_l . Through their individual decisions, they determine how to allocate the available power among themselves, based on their own preferences and objectives.

Charging Utility Function for EVs

Each EV player has a charging utility function $U_{e,i}(p_{e,i})$ that quantifies the satisfaction of the player or utility derived from obtaining a specific charging power $p_{e,i}$. The utility function is defined by the equation:

$$U_{e,i}(p_{e,i}) = Q_{e,i} \cdot p_{e,i}^{req} \cdot \ln(p_{e,i} + 1) \quad (2.35)$$

Here, $p_{e,i}^{req}$ represents the required charging power of the i th EV, and $Q_{e,i}$ is a parameter that reflects the EV's preference for charging. A larger $Q_{e,i}$ implies the EV is more urgent and desires faster charging. The natural logarithm function is common choice used to model the utility function design. The addition of 1 inside the logarithm prevents the utility from becoming undefined for zero charging power.

1. EV charging Preferences $Q_{e,i}$: The parameter $Q_{e,i}$ determines the EV's preference for charging. A higher $Q_{e,i}$ indicates a stronger urgency to charge quickly. EVs with smaller $Q_{e,i}$ values are more flexible and willing to share their allocated charging power to help other EVs with

higher urgency.

2. Maximizing Individual Utility: Each EV player aims to maximize its own utility by deciding how much charging power to allocate to itself. The utility function captures the trade-off between the obtained charging power and the EV's urgency for charging.

3. Total Charging Power Constraint: All EV players collectively compete for the total charging power p_l , which was determined in the first stage. The sum of the charging powers allocated to all EVs must be equal to the total charging power, as indicated by the equation:

$$\sum_{i \in I} p_{e,i} = p_l \quad (2.36)$$

4. EV Battery Dynamics: The dynamics of an EV battery's state of charge are described by the equation:

$$SOC_i(t+1) = SOC_i(t) + p_{e,i}(t)\Delta t\eta_{c,i}/E_{e,i} \quad (2.37)$$

Where, $p_{e,i}$ is the charging power for the EV, Δt is the time step, $\eta_{c,i}$ is the charging efficiency of the EV's battery, and $E_{e,i}$ is the battery capacity. This equation models how the SOC changes over time due to charging.

Generalized Nash Equilibrium

In this section the article explains the approach taken to address the EV charging coordination problem using a Generalized Nash Equilibrium (GNE) framework, involving the application of Karush-Kuhn-Tucker (KKT) conditions and the determination of the optimal charging powers for the EVs. A Generalized Nash Equilibrium (GNE) is a concept in a game theory that extends the traditional Nash equilibrium to situations where player strategy spaces are influenced by the strategies chosen by all other players. In a GNE, each player best response considers the strategies of all players simultaneously, rather than assuming that other player strategies are fixed. Consider the following Lagrangian functions:

$$L_i = -Q_{e,i} \cdot p_{e,i}^{req} \cdot \ln(p_{e,i} + 1) + \lambda_i \left(\sum_{i \in I} p_{e,i} - p_l \right) \quad (2.38)$$

and compute:

$$\frac{\partial L_i}{\partial p_{e,i}} = -\frac{Q_{e,i} \cdot p_{e,i}}{p_{e,i} + 1} + \lambda_i = 0 \quad (2.39)$$

- **Lagrangian Function and Gradient Condition:** Equation (2.38) defines the Lagrangian function L_i of the i th player, combining the utility function from equation (2.35) with the constraint term based on the total charging power constraint (2.36). Equation (2.39)

represents the gradient condition of the KKT optimality conditions, ensuring that the Lagrangian's derivative with respect to the charging power $p_{e,i}$ and the Lagrangian multiplier λ_i is zero.

- **Existence and Uniqueness of GNE:** Due to the convexity of the problem, the existence and uniqueness of the GNE can be proven mathematically. This means that the charging power allocation among EVs has a well-defined equilibrium point that satisfies both individual utility maximization and the total charging power constraint

$$\frac{Q_{e,i} \cdot p_{e,i}}{p_{e,i} + 1} = \bar{\lambda} \quad (2.40)$$

- **Socially Stable Equilibrium and $\bar{\lambda}$:** At the most socially stable equilibrium point, the relation (2.40) holds. This indicates a balance between the urgency for faster charging as expressed by $Q_{e,i}$ and $p_{e,i}^{req}$, and the Lagrange multiplier $\bar{\lambda}$, which represents the constraint of the total available charging power

$$p_{e,i} = \frac{Q_{e,i} \cdot p_{e,i}}{\bar{\lambda}} - 1 \quad (2.41)$$

- **Optimal charging Power Calculation:** Based on the value of $\bar{\lambda}$, the optimal charging power $p_{e,i}$ for the i th EV can be uniquely determined using equation (2.41). This equation calculates the charging power that satisfies both the utility maximization and constraint represented by λ .

$$0 \leq p_{e,i} \leq p_{e,i}^{req} \quad (2.42)$$

- **Charging Power Domain Constraint:** The optimal charging power (2.41) must be within the allowable domain, as indicated by equation (2.42). This constraint ensures that the calculated charging power is within the feasible range defined by the EV's required charging power $p_{e,i}^{req}$.
- **Centralized vs. Distributed Approach:** While a centralized approach could assign charging powers based on equation (2.41), it would require the centralized controller to have access to all EV information, which might not be privacy-preserving or flexible. Hence, the discussion points towards a distributed EV charging coordination algorithm that's more suitable for maintaining privacy and flexibility.

In summary, this section emphasizes the mathematical framework used to derive the optimal charging power allocations for EVs within GNE problem. It also contrasts centralised and distributed approaches, highlighting the advantages of a distributed approach in terms of privacy preservation and flexibility.

Distributed Implementation

Here, a distributed algorithm is described, named the consensus-network-based algorithm, proposed to solve the EV charging coordination problem. This algorithm leverages a communication network among EVs to coordinate their charging while considering both individual preferences and system constraints. Let's break down the key components of the algorithm as presented:

- **Algorithm Overview:** The algorithm is designed to facilitate the coordination of EV charging among multiple vehicles at a charging station. It is a distributed approach that utilizes a consensus network for communication and coordination.
- **Communication and Information Sharing:** Each EV initially publishes its necessary information, including the parameter λ_i and the required charging power $p_{e,i}^{req}$. The maximum charging power $p_{e,i}$ for each EV is determined by solving equation (2.35) under the constraint (2.42). This information is shared among the charging station and the neighboring EVs.
- **Charging Coordination in a Single EV case:** In the case where there is only one EV connected, the optimal dispatched charging power is simply set to $p_{e,i}=p_l$ reflecting the total available charging power.
- **Charging Coordination in Multiple EVs Case:** For the general case of multiple connected EVs, the algorithm proceeds as follows:
 - Power Mismatch Check (line 3): The difference between individual EV power $p_{e,i}$ and total available power p_l , i.e., $\Delta p = p_{e,i} - p_l$, is checked to determine system power balance.
 - Switch Variable LK (line 4): If the power balance condition is not met, the switch variable LK is set to 1, indicating that the consensus network needs to be initiated.
 - Consensus Network Interaction (line 5-7): Each EV interacts with its neighboring EVs through a consensus mechanism to update their individual parameter λ_i according to equation (2.43). This interaction helps the EVs collectively converge to a consistent λ_i value.

$$\lambda_i \leftarrow \lambda_i + \sum_{j \in N_i} w_{ij} (\lambda_j - \lambda_i) \alpha \Delta p \quad (2.43)$$

- Convergence check (line 8): Once the values of λ_i converges within a certain tolerance ε_1 , the switch variable LK is set back to 0.
- Decision update (line 10): Each EV then uses its updated λ_i to adjust its charging power decision $p_{e,i}$.

- GNE check (line 11): The power mismatch condition Δp is re-evaluated. If it is within a small tolerance ε_0 , the GNE of the problem is considered found. Otherwise the consensus process is repeated until the GNE is reached. Constraint violation (2.42) is also checked at each iteration.
 - Iteration (line 12): Since charging coordination is dynamic over time, the algorithm is repeated at each control time instant.
- **Local Information Utilization:** The algorithm solves the coordinated charging locally using information available to each EV. It utilizes the consensus mechanism to adjust λ_i and ensure coordinated charging among the EVs while respecting their preferences and system constraints

In summary, the proposed consensus-network-based algorithm enables a distributed coordination of EV charging using local information, communication among EVs, and a consensus mechanism to achieve a GNE solution while maintaining flexibility and privacy preservation. The algorithm solves in a distributed way the problem:

$$\max \sum_{i \in I} U_{e,i}(p_{e,i}), \text{ subjected to } \sum_{i \in I} p_{e,i} = p_l \quad (2.44)$$

Algorithm 2.2 : Distributed EV Charging Coordination.

- 1: **Initialization:** The plugged-in EV initialize $p_{e,i}^{req}$ and λ_i independently and receive p_l sent by the charging station.
 - 2: **if** EV charging number $N_{ev} \leq 2$ **then**
 - 3: **While** $\Delta p = |\sum p_{e,i} - p_l| > \varepsilon_0$ **do**
 - 4: $LK = 1$
 - 5: **Consensus Phase:** set up the consensus network.
 - 6: **while** ($\max(|\lambda_i - \lambda_j|) > \varepsilon_1$ or $LK = 1$) **do**
 - 7: $\lambda_i \leftarrow \lambda_i + \sum_{j \in N_i} w_{ij}(\lambda_j - \lambda_i)\alpha\Delta p$
 - 8: $LK = 0$
 - 9: **end while**
 - 10: $p_{e,i} = \frac{Q_{e,i} p_{e,i}}{\lambda} - 1$, and check (2.42)
 - 11: **end while**
 - 12: **else**
 - 13: $p_{e,i} = p_l$, and check (2.42)
 - 14: **end if**
-

Main Achievements:

In summary, the results of the proposed scheme yielded several significant achievements:

- **1. Power Allocation for EV Charging Demand Response:** The first stage of the proposed scheme successfully determined the optimal outputs of the PV, battery storage, and the grid supply. This approach led to a balanced compromise in the total charging power, optimizing the utilization of the battery to provide a consistent service and allowing for quick adjustments. As a result, the load on the grid was effectively reduced, contributing to a more sustainable and reliable power supply.
- **2. Grid Burden Reduction:** The utilization of the battery to manage EV charging demand resulted in a reduction of the overall burden on the grid. By intelligently allocating power between the PV system, battery, and the grid, the proposed scheme minimized the need for excessive grid supply during peak charging periods.
- **3. Quasi-Pricing Scheme for Peak Demand reduction:** The introduced quasi-pricing scheme played a pivotal role in lowering peak charging demand. By offering incentives and disincentives based on charging behaviors and demand patterns, the scheme incentivized to shift their charging times away from peak periods, contributing to more evenly distributed load on the grid.
- **4. EV Charging Coordination and Dispatch:** In the second stage of the proposed scheme, efficient EV charging coordination was achieved by distributing the available charging power among the EVs. The scheme considered individual preferences and urgent charging requirements, ensuring that EVs in need of immediate charging received higher priority for power allocation.
- **5. Enhanced Service and Flexibility:** The proposed scheme not only optimized grid utilization but also improved the service provided to EV owners. By effectively managing the battery resources and coordinating charging, the scheme offered long-lasting and reliable charging options to EV users while maintaining a level of flexibility to adapt to varying demand scenarios.

3

Power Distribution System Modelling

The studied system is an EV charging station connected to the grid, it is equipped with a PV source, a battery. Let T_s denote the sampling time and k as an index of discrete-time considered in this study. The charging station accommodates the stochastic and dynamic arrival of the various EVs. The arrived EV provides its charging requirements that are five parameters:

- Energy required (E_{req}): The energy that EV should have when leaving the station.
- Initial stored energy (E_{init}): The energy stored in the battery when EV reaches the station.
- Time of arrival (t_{arr}): The time instant EV reaches the station.
- Time of departure (t_{dep}): The time of departure declared by the EV owner.
- Flexibility (Flx) : expressed in percentage of the required energy that indicates how much the EV final stored energy can deviate from the required one.

The charging station acts as an energy supplier, providing the aggregate charging power for all EVs. This total charging power is sourced from a combination of the PV production, the battery, and the grid. The crucial aspect lies in determining the proportion of power supplied by each source. Due to the limited power capacity, the charging station might encounter challenges in fulfilling the desired charging requirements of all EVs. In such cases, some EVs may not receive their full requested charge.

3.1 BATTERY MODEL

1)Parameters

- E_b^{max} : The maximum energy that the battery can store (maximum capacity).
- E_b^{min} : The minimum energy that the battery should maintain.
- $E_{b,Opt}$: The preferred stored energy that the battery should have.
- P_b^{min} : The minimum power of the battery.
- P_b^{max} : The maximum power of the battery.
- $SOC_b^{min} := \frac{E_b^{min}}{E_b^{max}}$: The minimum state of charge of the battery
- $SOC_b^{max} := 1$: The maximum state of charge of the battery.
- $SOC_{b,Opt} := \frac{E_{b,Opt}}{E_b^{max}}$: The preferred state of charge that should the battery have.

2)Variables

- $E_b(k)$: The energy stored in the battery at time k .
- $SOC_b(k) := \frac{E_b(k)}{E_b^{max}}$: The state of charge of the battery expressed in terms of percentage of the maximum energy at time k .
- $P_b(k)$: The power flow of the battery at time k .

3)Dynamic Model Of The Battery The stationary storage battery functions as an energy buffer for both the PV and the grid. It generates a power $P_b(k)$ and has maximum capacity energy E_b^{max} . ESS is modelled as dynamic discrete-time system:

$$E_b(k + 1) = E_b(k) + P_b(k)T_s \quad (3.1)$$

It is better to express the state of charge of the battery in terms of percentage of the maximum capacity. Hence, dividing (3.1) by $E_{b,max}$, we obtain:

$$SOC_b(k + 1) = SOC_b(k) + P_b(k)T_s/E_{b,max} \quad (3.2)$$

where $SOC_b(k)$ is the state of charge of the battery at time k . The battery can supply power to the network and also absorb power from it. In other words, it can act as both an energy source

and an energy sink, depending on the current requirements of the system. When the power is negative, it means that the battery is discharging, when the power is positive, it means that the battery is charging.

4) Constraints On The Battery

To prevent the battery degradation and ensure its longevity, the stored energy $E_b(k)$ should not go below a certain minimum E_b^{min} , and has to stay below the capacity E_b^{max} , namely:

$$E_b^{min} \leq E_b(k) \leq E_b^{max} \quad (3.3)$$

By dividing by E_b^{max} , we obtain constraint on state of charge:

$$SOC_b^{min} \leq SOC_b(k) \leq SOC_b^{max} \quad (3.4)$$

The battery has both a maximum power output and a minimum power absorption capacity (P_b^{max} , P_b^{min}). The charging station management system must consider these limits to ensure that the battery operates within its safe and efficient operational range. Hence, we impose:

$$P_b^{min} \leq P_b(k) \leq P_b^{max} \quad (3.5)$$

5) Cost function of the battery

The cost function of the battery will be the summation of three terms over the prediction horizon T_H :

$$C_b = C_{b1} + C_{b2} + C_{b3} \quad (3.6)$$

where:

$$C_{b1} = w_1 \sum_{k=0}^{T_H} P_b^2(k) \quad (3.7)$$

$$C_{b2} = w_2 \sum_{k=0}^{T_H} (SOC_b(k) - SOC_{opt})^2 \quad (3.8)$$

$$C_{b3} = w_3 \sum_{k=0}^{T_H} (P_b(k) - \frac{1}{T_H} \sum_{k=0}^{T_H} P_b(k))^2 \quad (3.9)$$

The weighting factors, denoted as w_1 , w_2 and w_3 are employed to assign varying levels of importance to the distinct terms.

- The first term C_{b1} represents the cost associated with the battery usage, whether it is in

charging mode or discharging mode. By imposing a cost every time the battery is used, the system will explore an alternative ways to meet its energy needs without relying on the battery. The idea is to strike a balance between using the battery when it is necessary, and avoiding unnecessary use to prolong its operational life and minimize expenses.

- The second term C_{b2} represents a cost associated with the deviation of the battery's SOC from its optimal level. It is preferable to keep the battery in a specific optimal state of charge ($SOC_{b,Opt}$). By doing so, the battery can promptly discharge or absorb power, allowing it to offer a significant regulation margin for rapid adjustments when necessary. This ensures the battery's ability to provide adequate and timely power delivery or absorption as needed. The cost will rise whenever the battery's state of charge is either below or above the optimal level.
- The third term C_{b3} characterizes the expense linked to battery's behaviour. To maintain the battery life time and ensure its optimal performance, it is essential to avoid excessive charging and discharging. Frequent and rapid switching between charging and discharging states can damage the battery. This phenomenon is known as "cycling" and is a major factor affecting the lifespan of rechargeable batteries. During each charge and discharge cycle, the battery materials expand and contract, leading to mechanical stress and chemical changes. Over time, these stresses and changes can result in the gradual breakdown of the battery electrodes and electrolyte, causing a decrease in its capacity and overall performance. In this case the cost will be increased, thus, the system try to uphold a consistent battery power over extended periods rather than subjecting it to rapid and varying power changes.

3.2 EV MODEL

1)Parameters

EV battery has the same characteristics as the ESS. In addition, we associate five other parameters provided by each EV owner. These parameters will be an input to our optimizer. First we assume that the i th EV arrives at the station at the arrival time $t_{arr,i}$, and leaves the station at the departure time $t_{dep,i}$. Second, we assume that the stored energy of the i th EV battery at arrival time is $E_{init,i}$ while the required stored energy at departure time is $E_{req,i}$. Third, we assume that the energy required at the departure time is smooth and we introduce a flexibility index (Flx_i), it is a percentage of how much the consumer of the i th EV is flexible about his state of charge at departure time. The remaining characteristics are:

- $E_{EV,i}^{max}$: The maximum energy that the i th EV battery can store (maximum capacity).
- $E_{EV,i}^{min}$: The minimum energy that should not the i th EV battery goes below.
- $SOC_{EV,i}^{min} := \frac{E_{EV,i}^{min}}{E_{EV,i}^{max}}$: The minimum state of charge of the i th EV battery.
- $SOC_{EV,i}^{max} := 1$: The maximum state of charge of the i th EV battery.
- $E_{init,i}$: The initial energy stored in the i th EV when it arrives at the station.
- $SOC_{init,i} := \frac{E_{init,i}}{E_{EV,i}^{max}}$: initial state of charge when the i th EV arrives at the station
- $P_{EV,i}^{min}$: The minimum power flow of the i th EV battery.
- $P_{EV,i}^{max}$: The maximum power flow of the i th EV battery.
- $E_{req,i}$: The required energy to be stored in the i th EV when it leaves the station.
- $t_{arr,i}$: The time at which the i th EV arrives at the station.
- $t_{dep,i}$: The tile at which the i th EV leaves the station.
- flx_i : Flexibility index for the i th EV.

2) Variables

- $E_{EV,i}(k)$: Energy stored in the i th EV battery at time k .
- $SOC_{EV,i}(k) := \frac{E_{EV,i}(k)}{E_{EV,i}^{max}}$ State of charge of the i th EV battery at time k .
- $P_{EV,i}(k)$: The power of the i th EV battery at time k .

3) **Dynamic Model** The dynamics of the i th EV battery is:

$$E_{EV,i}(k+1) = E_{EV,i}(k) + P_{EV,i}(k)T_s \quad (3.10)$$

The energy stored in the battery as percentage of the maximum capacity is as follows :

$$SOC_{EV,i}(k+1) = SOC_{EV,i}(k) + P_{EV,i}(k)T_s/E_{EV,i}^{max} \quad (3.11)$$

4) Constraints

We impose some operational constraints on the EV battery that should be respected. Energy

stored in the battery should not go below a certain minimum $E_{EV,i}^{min}$, and has to stay below its maximum capacity $E_{EV,i}^{max}$, namely:

$$E_{EV,i}^{min} \leq E_{EV,i}(k) \leq E_{EV,i}^{max} \quad (3.12)$$

Dividing by $E_{EV,i}^{max}$ we get the constraint on the state of charge:

$$SOC_{EV,i}^{min} \leq SOC_{EV,i}(k) \leq SOC_{EV,i}^{max} \quad (3.13)$$

EVs are capable of both absorbing and supplying power to the network, which is known as bidirectional capabilities. When the power of EV is negative means it is providing energy, when it is positive means it is charging. We impose that:

$$P_{EV,i}^{min} \leq P_{EV,i}(k) \leq P_{EV,i}^{max} \quad (3.14)$$

In real-world scenarios, it may not always be possible to fulfill the energy requirements of EV consumers precisely based on their desired charging patterns or grid conditions. To address this variability and uncertainty, a flexibility index is introduced in the departure time. The Energy stored at the departure time will have the following constraint:

$$(1 - Flx_i)E_{req,i} \leq E_{EV,i}(t_{dep,i}) \leq E_{req,i} \quad (3.15)$$

Hence, the state of charge at departure time will have the following constraint:

$$(1 - Flx_i)SOC_{req,i} \leq SOC_{EV,i}(t_{dep,i}) \leq SOC_{req,i} \quad (3.16)$$

where $E_{EV,i}(t_{dep,i})$ and $SOC_{EV,i}(t_{dep,i})$ is the energy stored and state of charge at departure time of the i th EV respectively.

5) The cost function of EVs

The cost function of the EVs that will contribute to calculate the total cost function depends on the how much the consumer is satisfied, in other word how much the final state of charge will be near to the required state of charge:

$$C_{EV} = w_5 \sum_{i=1}^{N_{EV}} (SOC_{EV,i}(t_{dep,i}) - SOC_{req,i})^2 \quad (3.17)$$

Where N_{EV} is the total number of EV arrived in the time horizon T_H . w_5 is a waiting factor expressing the degree of interest in achieving the desired energy level of EVs.

3.3 PV MODEL

1)Parameters

- A_{PV} : PV panel surface.
- η_{PV} : The conversion efficiency.

2)Variables

- $P_{PV}(k)$: Real PV power production.
- $\hat{P}_{PV}(k|t)$: Predicted PV power production at time k given t real past samples of PV power production.
- $\hat{P}_{PVN}(k)$: predicted PV power production in sunny day (nominal prediction).
- $G_i(k)$: is the solar irradiance at time k .

3)Model of PV

Typically, PV panels are presumed to operate at the maximum power mode, and an approximated estimation of the corresponding power can be obtained by:

$$P_{PV}(k) = G_i(k)A_{PV}\eta_{PV} \quad (3.18)$$

Where A_{pv} is the installed PV panel surface area, $G_i(k)$ is the solar irradiance at time k and η_{pv} is the conversion efficiency. Solar irradiance directly impacts the performance of PV panels, and its levels are heavily dependent on weather conditions. The amount of sunlight received by the PV panels affects their electricity generation capacity. On sunny days with high solar irradiance, the PV panels produce more energy, while on cloudy or overcast days with lower solar irradiance, their output will be reduced. Similarly, factors like shading, dust, and other environmental conditions can also influence the overall solar irradiance, consequently, the efficiency of the PV panel. As a result of these uncertainties, the prediction of the PV power generation becomes more complex. However, we can improvise to update the expectation power based on real production and give better expectation in the remaining period of the day. Suppose we

are at sampling time t , at the current sampling time, we have gathered a total t actual samples of PV power generation. Up to this point, the predicted PV power values have consistently differed from the actual values. Our objective is to enhance the accuracy of future PV power prediction by leveraging this historical real-data.

Where $\hat{P}_{PVN}(j)$ is the expectation of PV power production based on the weather, $P_{PV}(j)$ is the real PV production and $\hat{P}_{PV}(k|t)$ is the updated expectation of PV power for each $k \geq t$, which is based on combination of real production and weather expectation.

4)Constraint and cost

It is clear that the total cost function for optimization will not depend on the PV, because the PV is expected to give its total power, so there will be neither a cost nor a constraints based on PV parameters.

3.4 GRID MODEL

1)Parameters

- P_g^{max} : The maximum power that can be exchanged between the grid and the EV station.
- P_g^{min} : The minimum power that can be exchanged between the grid and the EV station.

2)variables

- $P_g(k)$: The power exchanged between the grid and the EV station at time k .

The cost of power from the grid refers to the monetary expense associated with drawing electricity from the utility grid to meet the energy demand. It is common for grid operators to charge consumers based on the amount of electricity they consume. The cost of grid electricity can vary based on several factors, for example the time of use, in which electricity costs more during peak demand periods (typically during daytime) and less during off-peak hours (at night).

3)Constraints of the grid The grid typically has limitations on the minimum and maximum power that can be exchanged with the network. These constraints are important to ensure the stability and reliability of the grid system. We impose:

$$P_g^{min} \leq P_g(k) \leq P_g^{max} \quad (3.19)$$

Where $P_g(k)$ is the power exchanged by the grid and the station, and it can be negative or positive. When it is negative the grid is buying energy, when it is positive the grid is selling energy.

4) The cost of the grid

The cost function of the grid is as follows:

$$C_g = w_4(k) \sum_{t=0}^{T_H} P_g(k) \quad (3.20)$$

Where $w_4(k)$ is a varying waiting factors that varies depending on the time of the day, for example the waiting factor is greater at the peak time than at the normal time. This is a strategy used to shift energy-intensive tasks to a non-peak hours. This can involve scheduling heavy energy use activities during times when electricity demand is lower, reducing the overall electricity costs. From the cost function, it is clear that it is not preferable to use the power of the grid, and also it encourage to sell or give power to the grid, when the grid take power from the customer, means that $P_g(k)$ is negative, which reduces the cost.

4

MPC-Based Centralised Power Control Design

Model predictive control represents a sophisticated model-based control approach designed to optimize a system behaviour over a future time horizon, taking into consideration the future prediction of the system. During each sampling time, this predictive control method calculates the control signal by minimizing a cost function over a predictive horizon while considering operational system constraints. However, only the initial input of the signal is used for that sample time. Afterward, the model state is updated, and the optimization process is repeated over the same horizon time or reduced horizon time depending on the application, or on the complexity of the system. The time complexity of MPC can vary depending on various factors, including the prediction horizon, the complexity of the system model, and the used optimization algorithm. As the prediction horizon increases, the complexity of the optimization problem grows, leading to higher computational demands. Different optimization algorithms have different complexities. For example, linear quadratic regulators (LQR) have a quadratic time complexity, while more advanced optimization techniques like quadratic programming (QP) and non linear programming (NLP) have higher time complexity. The dependence of time complexity on the sampling time used in MPC is not direct. The sampling time defines the rate at which the control inputs is updated and the system state is measured. A smaller sampling time allows for more frequent control updates, which can improve the control performance, and consequently the stability of the system. However, it also increases the computational

burden since the MPC needs to solve the optimization problem more frequently. In practice, engineers and researchers often choose an appropriate sampling time that strikes a balance between control performance and computational efficiency based on the specific requirements of the controlled system. Our optimization problem involves making decisions regarding how to distribute energy resources over the upcoming day. The goal is to minimize costs while also ensuring a consistent and reliable energy supply. Depending on the chosen sampling time and cost function, the time required to solve the optimization problem will vary. For instance, if the sampling time is set to 15 minutes, there will be 96 samples in a day, and the optimization problem has to be solved in less than 15 minutes. However, this large sampling period may result in a reduced system performance. Furthermore, if an EV arrives during the sampling period, the optimization problem does not incorporate it into the calculation until the subsequent sampling period, resulting in a noticeable delay. On the other hand, decreasing the sampling time to 1.5 min would yield to 960 samples, thus, the OP has to be solved in a time less than 1.5 min. However, solving the optimization problem with such sampling time would take more than 2 minutes, rendering the problem infeasible. This is particularly challenging when the control decisions must be updated every 1.5 minute. In our study, it is not necessary to update the control decisions every minute at the start of the day when there is neither PV production nor any EVs plugged in. However, as soon as EVs begin to arrive or the PV system initiates power generation, the control decisions need to be promptly updated. To simplify the time complexity, one approach is to adopt a reduced time horizon that encompasses this particular period.

In MPC the control decision is made based on model prediction, that in our case is the prediction of PV power production. We are also interested in predicting the EVs Model.

4.1 MODELLING METHODOLOGY

In this section, we establish the synthetic data generator (SDG). The SDG is characterized as a parametric model capable of producing an instance of EVs data. Our assumption is that the attributes of each instance can be encapsulated using three parameters:

- The arrival time.
- The connection time.
- The required energy.

The departure time can be computed directly as the summation of the arrival time and the connection time. In order to generate data, we pass through the following two step process:

- **Step 1:** We create the EV arrival times within the specified input time frame. This time frame, known as the horizon time, represents the duration over which data generation is required.
- **Step 2:** After obtaining the EV arrivals, we proceed to generate the corresponding connection time and required energy for each individual EV.

4.1.1 ARRIVALS MODEL

In various real-world scenarios, understanding the patterns of events occurrence is essential for an effective planning and decision-making. One common scenario involves the arrival of cars at a certain location, such as a parking lot or a drive-thru. This arrival pattern can be modelled using probability distributions. The Poisson distribution is a fundamental probability distribution used to describe the number of events that occur within a fixed interval of time or space. It is particularly useful when events occur randomly and independently at a certain rate. For example, if we are interested in understanding how many cars arrive at a specific location within an hour, the Poisson distribution can provide the likelihood of different arrival counts. To simulate this scenario, we can pair the Poisson distribution with the uniform distribution. The uniform distribution ensures that events, in this case, car arrivals occur at random times within a fixed interval. By combining these distributions, we can generate a realistic model of car arrival. This simulation approach allows us to experiment with a different parameters, analyzing arrival patterns, and make informed predictions about the number of cars and their arrival times.

Arrival Count Model

We divide the time horizon $[0, T]$ into time slots, which has specific length, denoted as Δt . Our attention is directed towards producing the count of arrivals within a designated time slot t_s . The count of arrivals, denoted as N in t_s is simulated by selecting a random sample from a discrete probability distribution. Assuming that N follows a Poisson distribution model characterized by a parameter λ .

$$\lambda = f(t_s) \tag{4.1}$$

$$P(N = K) = \frac{e^{-\lambda} \lambda^K}{K!}, K = 0, 1, 2, \dots \quad (4.2)$$

where:

- N : The random variable representing the number of EVs arrived at a given time slot t_s .
- K : A specific value of the random variable.
- λ : The average rate of EVs arrival at given time slot.

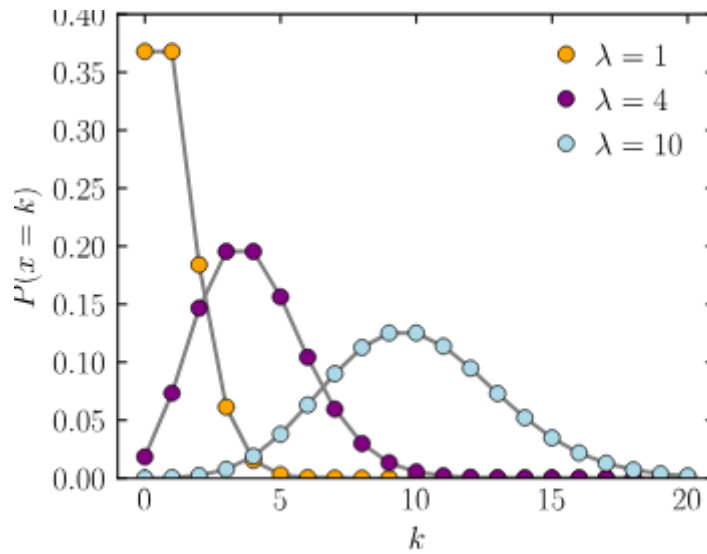


Figure 4.1: Probability distribution function of Poisson distribution.

From fig(4.1) taken from Wikipedia:

- As λ increases, the distribution shifts to the right. This means that as the average rate of EVs increases, the expected number of EVs in a fixed interval also increases.
- When λ is small the distribution is more concentrated around lower values. The expected number of EVs will be smaller.

Algorithm (4.1) outlines the procedure for calculating the number of EVs in a given time slot t_s . Initially, we fix an average rate for each specific time slot, as shown in equation (4.1). Subsequently, the EV count for that particular time slot is generated utilizing a Poisson distribution using the previously assigned average rate. This sequence of steps is iterated for every time slot throughout the day.

Algorithm 4.1 Number of arrival EVs

Input t_s : time slots period within a day.

Output N: Number of arrival EV.

for $t_s = 1, \dots, 24$.

$\lambda = f(t_s)$.

N = sample from Poisson distribution with rate λ .

Set N number of EV in time slot t_s .

Arrival Times Model

For the purpose of representing the arrival times ($t_{arr,i}$), we employ the uniform distribution, that has a constant probability density function over an interval $[0, \Delta t]$.

$$PDF(t_{u,i}) = \begin{cases} \frac{1}{\Delta t}, & 0 \leq t_{u,i} \leq \Delta t \\ 0, & otherwise \end{cases} \quad (4.3)$$

$$t_{arr,i} = (t_s - 1) + t_{u,i} \quad (4.4)$$

where PDF denotes a probability distribution function, $t_{u,i}$ follows a uniform distribution with interval $[0, \Delta]$, means that $t_{u,i}$ can take any number in the interval $[0, \Delta t]$ with the same probability. $t_{arr,i}$ is the arrival time of the i th EVs that arrives in the time slot t_s . I.e. In every equation, the time variable should always converted to the same unit.

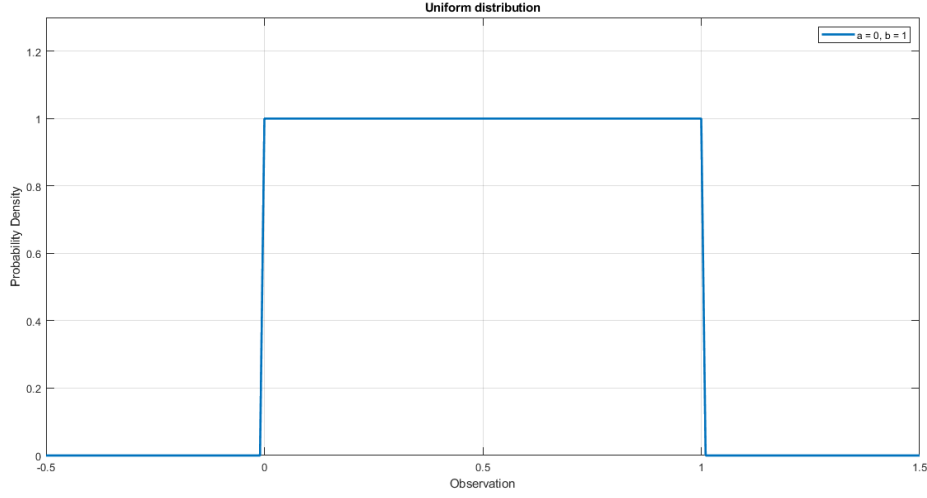


Figure 4.2: Probability distribution function of uniform distribution.

Algorithm 4.2 Arrival time

Input t_s : period within a day.

N: number of EV in this time slot.

Output $t_{arr,i}$ arrival time of each EV.

for $t_s = 1, \dots, 24$.

1) generate $t_{u,i}$ from the uniform distribution for each EV in time slot t_s .

2) Set $t_{arr,i} = (t_s - 1) + t_{u,i}$.

Energy required and Connection Time generation

The energy required and the connection time of the EV are generated as an independent random variable.

- We consider the case where EVs arrive to the station with a low SOC. Let SOC_H be a certain high SOC, for example we can set it as 0.7. We generate the expected SOC required ($SOC_{req,i}$) for each EV randomly around this level (SOC_H) using uniform distribution.

$$SOC_{req,i} \sim U[0.9SOC_H, 1.1SOC_H] \quad (4.5)$$

- We consider a specific scenario in which the EVs will stay at the station for a long period. Depending on the capacity and the maximum power of the EV's battery, we can calculate the minimum necessary time t_{min} to fully charge the EV battery. We set the connection time $t_{c,i}$ of the i th EV to be greater than this period and to be less than a maximum time t_{max} .

$$t_{c,i} \sim U[t_{min}, t_{max}] \quad (4.6)$$

The time of departure $t_{dep,i}$ can be calculated as follows:

$$t_{dep,i} = t_{arr,i} + t_{c,i} \quad (4.7)$$

4.1.2 PV ADAPTATION METHOD

The predicted PV power production at time k given t real past samples of PV power production.

$$\hat{P}_{PV}(k|t) = \frac{\sum_{j=0}^t P_{PV}(j)}{\sum_{j=0}^t \hat{P}_{PVN}(j)} \hat{P}_{PVN}(k) \quad (4.8)$$

Where $\hat{P}_{PVN}(j)$ is the expectation of PV power production based on the weather, $P_{PV}(j)$ is the real PV production and $\hat{P}_{PV}(k|t)$ is the updated expectation of PV power for each $k \geq t$, which is based on combination of the real production and the weather expectation.

4.2 OPTIMIZATION PROBLEM METHODOLOGY

Notation

- T_s : The sampling time.
- T : The number of sample in one day with sampling time T_s .
- T_H : The time horizon used in the OP.
- t_u : The time in which real EVs start to arrive, or the PV starts to produce power.

- \hat{N}_{EV} : The total expected number of EV arrived in all the day.
- \hat{T}_{ad} : A $(\hat{N}_{EV} \times 2)$ matrix in which first column contains times of arrival, second column contains the corresponding times of departure for expected model.
- \hat{E}_{req} : A (\hat{N}_{EV}) dimensional vector contains the energies required for every EV in the expected model.

- $\hat{S} = \{ \hat{D}_1, \hat{D}_2, \dots, \hat{D}_{\hat{N}_{EV}} \}$
- $\hat{D}_i = \{ \hat{E}_{init,i}, \hat{E}_{req,i}, \hat{t}_{arr,i}, \hat{t}_{dep,i} \}$

At time t during the day where real time data is available, we split the expected data set into two sets:

- $\hat{S} = \hat{S}_t^- \cup \hat{S}_t^+$
- $\hat{S}_t^- = \{ \hat{D}_i \in \hat{S} | \hat{t}_{arr,i} \leq t \}$
- $\hat{S}_t^+ = \{ \hat{D}_i \in \hat{S} | \hat{t}_{arr,i} > t \}$

- N_{EV} : The total number of real EV arrived in all the day.
- T_{adv} : A $(N_{EV} \times 2)$ matrix contains the real times of arrival and times of departure.
- E_{reqr} : A (N_{EV}) dimensional vector contains the energies required for every EV in the real model.

At the end of the day we will have the real data set:

- $S = \{ D_1, D_2, \dots, D_{N_{EV}} \}$
- $D_i = \{ E_{init,i}, E_{req,i}, t_{arr,i}, t_{dep,i} \}$

We split the real data set into two sets:

- $S = S_t^- \cup S_t^+$
- $S_t^- = \{ D_i \in S | t_{arr,i} \leq t \}$
- $S_t^+ = \{ D_i \in S | t_{arr,i} > t \}$

We consider the variable inputs for the optimizer:

- Nu_{EV} : is the summation of the actual number of EV in the station and the expected EV to be arrived in future time.

- T_{adu} : is a matrix obtained by combining \hat{T}_{ad} and T_{adr} , the first part of this vector contains the updated information when real data is available, while keeping the expected information of the future time.
- $Erequ$: is a mixed vector of $\hat{E}req$ and $Ereqr$, the first part of this vector contains the updated energy required when real data is available, while keeping the expected energy required for future expected arrival EVs.

We define the set over which we perform the optimization at time t .

- $\bar{S}_t = S_t^- \cup \hat{S}_t^+$

We can split the OP into two parts:

- The first part we consider the OP before real EVs start to arrive and before the real PV production. In other words, we consider the OP taking into consideration only the expected models. In this case, $\bar{S} = \hat{S}$
- The second part we consider the OP when the real EVs start to arrive or when PV start to generate power. In this case, we have to incorporate the expected data with the real data. Thus, $\bar{S}_t = S_t^- \cup \hat{S}_t^+$

Part 1:

The role of this part is to give an initial control decision. For example we know that the power demand will be high at the arrival of EVs, thus the battery has to be charged before that time. Or, if there will be a surplus of energy when the PV starts to produce power, the battery needs to be discharged in order to capture this excess of energy. Since the OP is based only on the predicted model, we can address the situation by solving a single optimization problem based on the expected model, considering the predicted EV arrival and departure times, the energy requirements for each EV, and the predicted PV production. As there is no new data, there is no need to update the control decision every 1.5 minute in this part. This unchanged control decision remains valid until the first EV arrives, or when the PV start to generate power in real time. Subsequently, as more EVs start arriving, the model needs updating, leading to adjustments in the control decision. Even if solving the optimization problem takes more than 1.5 min, in this part, it does not pose a problem since the control decision does not have to be updated each 1.5 minute.

Part 2:

This part initiates when real EVs start to arrive. In this case, the OP must take into consideration the available real data. For example, we are expecting the PV to generate a certain amount of energy. But, in reality, it generates different amount. In this case the OP problem will be changed, and the control decisions will be changed accordingly. The same thing is for EVs. If we expect that a certain number of EVs will arrive at a given period, in reality, different number of EVs will arrive. In this part, the OP problem has to be solved every minute, and the control decisions will be updated accordingly. At this point, the time horizon will be reduced, and consequently also the complexity of the system will be reduced, so that the time needed to solve the problem will be feasible.

In the first part, the cost function to be optimized over the set \hat{S} is as follows:

$$\min_{U(0:T)} C_{Tot} = C_b + C_g + C_{EV} \quad (4.9)$$

Under the constraints:

$$C_b = \sum_{k=0}^T w_1 P_b^2(k) + w_2 (SOC_b(k) - SOC_{opt})^2 + w_3 \left(P_b(k) - \frac{1}{T_H} \sum_{k=0}^T P_b(k) \right)^2 \quad (4.10)$$

$$C_g = \sum_{k=0}^T w_4(k) P_g(k) \quad (4.11)$$

$$C_{EV} = \sum_{i=1}^{Nu_{EV}} w_5 (SOC_{EV,i}(t_{dep}) - SOC_{dep,i})^2 \quad (4.12)$$

$$P_b(k) + \sum_{i \in Nu_{EV}} (P_{EV,i}(k)) = P_g(k) + P_{pv}(k) \quad (4.13)$$

- $U(k) = [P_g(k), P_b(k), P_{EV,i}(k)]$, ($i \in Nu_{EV}$, $k = 0, \dots, T$), represents the set of controllable variables.

The inputs for the MPC in the first part are: $T_{adu} = \hat{T}_{ad}$, $E_{requ} = \hat{E}_{req}$, $Nu_{EV} = \hat{N}_{EV}$, $\hat{P}_{PV} = \hat{P}_{pvN}$, and the time horizon T_H .

The control decisions obtained from the solution of the first OP are applied until the time t_u that denotes the time of the first actual arrives EV, or the time at which the PV starts power production. In other words, t_u is the time when a new data is available, and hence an update

has to be done.

In the second part The optimizer input should be updated every minute. Consequently, the OP needs to be solved at each update over the set \bar{S}_t , yielding control decisions for current time. The new cost function will be as follows:

$$\min_{U(k:T)} C_{Tot}(k) = C_b(k) + C_g(k) + C_{EV}(k) \quad (4.14)$$

Under the constraints:

$$C_b(k) = \sum_{j=k}^T w_1 P_b^2(j|k) + w_2 (SOC_b(j|k) - SOC_{opt})^2 + w_3 (P_b(j|k) - \frac{1}{T_H} \sum_{j=k}^T P_b(j|k))^2 \quad (4.15)$$

$$C_g(k) = \sum_{j=k}^T w_4 P_g(j|k) \quad (4.16)$$

$$C_{EV}(k) = w_5 (SOC_{EV,i}(t_{dep}) - SOC_{dep,i})^2 \quad (4.17)$$

Where k is the current time. It is clear that the time horizon for the optimization problem is reduced by k , $T_H = T - k + 1$. At this time, we look for a variable sequence of $U(k|k)$, $U(k + 1|k)$, \dots , $U(T|k)$ that minimize C_{Tot} in equation (4.3). We put $U(k) = U_{k|k}$, we repeat the operation for $k = k + 1$ over shorter variable sequence $U(k + 1|k + 1)$, $U(k + 2|k + 1)$, \dots , $U(T|k + 1)$. We repeat the operation again until $k = T$.

Algorithm 4.3 MPC-based controller algorithm

Initialization

1) consider optimization problem (4.10). Set the Input of the optimizer to:

$$T_{adu} = \hat{T}_{ad}, Ereq_u = \hat{E}req, Nu_{EV} = \hat{N}_{EV}, \hat{P}_{PV} = \hat{P}_{pvN}$$

2) solve optimization

Set the control decisions $U(k)$, for $k=0, \dots, t_u$

Adaptation

2) for $k=t_u, \dots, T$

3) update the input of the optimizer

$$4) T_{adu} = [T_{ad}(k); \hat{T}_{adr_k}^+], Ereq_u = [Ereq(k); \hat{E}req_k^+], Nu_{EV} = N_{EV}(k) + \hat{N}_{EV}, \hat{P}_{PV}(k|t) = \frac{\sum_{j=0}^t P_{PV}(j)}{\sum_{j=0}^t \hat{P}_{PVN}(j)} \hat{P}_{PVN}(k)$$

7) solve the optimization problem (4.15) with the updated inputs.

8) set the control decision $U(k)$, which is the first element in the solution of the OP.

9) update SOC of the battery.

10) update state of charge of every EV.

5

Implementation And Simulation Setup

In this section, we provide simulation test results to demonstrate the effectiveness of the proposed control approach. The tests show the benefits gained from the incorporation of the adaptive optimizer when updating the new data. Additionally, we highlight the advantages of reducing the time horizon, which significantly contributes to both simplifying the system's complexity and enhancing its overall performance. Additionally, we explore the integration of the EVs in the network. We show how the control discharges the EV batteries during the peak demand periods. This can help to reduce the need for expensive peaking power plants and decrease the strain on the grid, leading to a cost savings and an improved grid reliability.

First, we evaluate the control approach ability to adapt the optimizer when new data become available. Traditional control methods often struggle with accommodating changes in the underlying system dynamics. However, our proposed approach leverages an adaptive optimizer that can seamlessly integrate the new data, enabling the system to remain effective in a dynamically changing environments. The simulation results illustrate the improved performance achieved through this adaptation process, reinforcing the control approach robustness and adaptability.

Second we investigate the effects of reducing the time horizon on the system's performance and complexity. By reducing the prediction horizon, we are able to significantly simplify the computation demands of the control approach. This reduction in complexity translates into

faster computation times and more efficient real-time control, providing valuable insights into system's behaviour under different settings.

Overall, the simulation tests provide strong evidence of the advantages offered by the proposed control. The adaptability of the optimizer to new data and the optimization of the time horizon demonstrate how the approach addresses challenges posed by changing environments while maintaining the system efficiency.

5.1 EV PARAMETERS

As discussed in previous section, we used Poisson distribution with time varying average to model the number of EVs arrival. The average number of EV arrived will differ in each time slot. The simulation time is one day, with sampling time $T_s = 1.5 \text{ min}$. The length of each time slot $\Delta t = 60 \text{ min}$

t_s	7	8	9	10	11	12	13	14	15	16	17	18
$\lambda(t_s)$	2	3	5	6	7	8	7	6	5	4	3	2

Table 5.1: Rate of the EVs arrival with the Poisson distribution model

From table (5.1), we record different averages for different time slots. The peak hours have greater average (8 EVs per hour), while other times have less average (2 EVs per hour).

We set the same parameters for the battery of EVs :

$E_{EV,i}^{max}$	$E_{EV,i}^{min}$	$SOC_{EV,i}^{max}$	$SOC_{EV,i}^{min}$	$P_{EV,i}^{max}$	$P_{EV,i}^{min}$	flx_i	t_{min}	t_{max}	SOC_H
40 KWh	0 KWh	1	0	14 KW	-14 KW	10 %	300 min	360 min	0.7

Table 5.2: EVs battery parameters and constraints

Table (5.2) summarizes the operational constraints of the EVs battery. We used $14kW$ for the power of the battery because 88% of charging points are between $7.4KW$ and $22KW$. The capacity of the battery is $40KWh$. In order to fully charge the battery with maximum power we need $2.8h$. Hence the minimum time in which EVs will use the charging points will be greater than $2.8h$

EVs setup

- Set the length of time slot $\Delta t = 1 \text{ h} = 60 \text{ minutes}$.
- Generate the expected arrival EVs in each time slot using algorithm (4.1).
- Generate the time of arrival of each EV using algorithm (4.2).
- Generate randomly the connection time that each expected EV is going to stay at the charging point in the interval from 5 hours to 6 hours. Thus, each EV can be used as source when there is lack of energy. From the connection time of the EVs, we deduce the departure time using equation (4.8).
- Round the arrival time and departure time according to the sampling time.
- Generate randomly the required energy for each expected EV between 24 KWh and 32 KWh . which means the state of charge will be between 0.6 and 0.8.
- We do the same procedure to generate the real data (the real number of EVs, its arrival times, departure times, required energies).

5.2 BATTERY PARAMETERS

E_b^{max}	E_b^{min}	SOC_b^{max}	SOC_b^{min}	P_b^{max}	P_b^{min}	$E_{b,Opt}$	$SOC_{b,Opt}$
400 KWh	80 KWh	1	0.2	60 KW	-60 KW	200 KWh	0.5

Table 5.3: ESS battery parameters and its constraints

The capacity of the battery is 400 KWh which can charge more than 10 EVs, the maximum power of the battery is 60 KW , it can give a support to the grid for more than 4 EVs. We set the optimal state of charge to 50%, which gives a good margin to the battery to discharge when there is a lack of energy and to charge when there is a surplus of energy.

5.3 GRID PARAMETERS

We set the maximum power that can the grid provides to the network to $P_g^{max} = 100 \text{ KW}$ and the minimum power to $P_g^{min} = -100 \text{ KW}$.

5.4 PV PARAMETERS

We take the PV data from IEEEPES (Power And Energy Society) for a two different days.

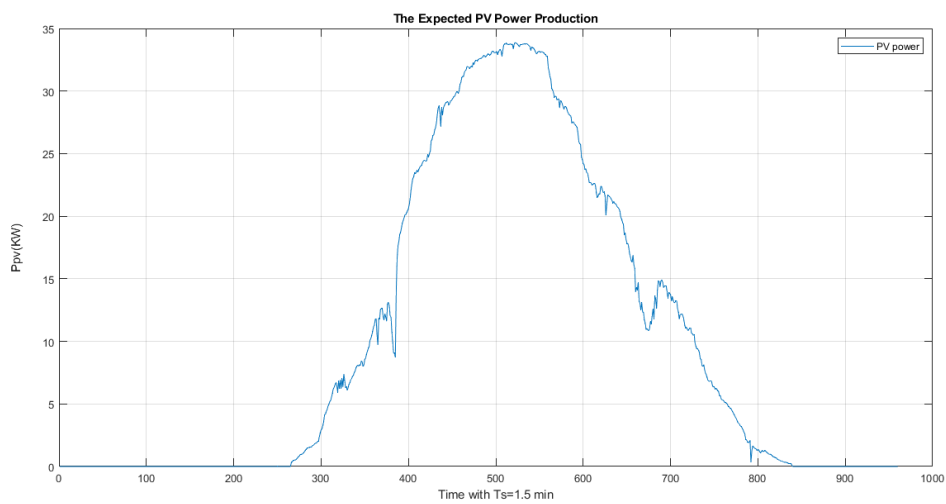


Figure 5.1: The expected PV Power production for a sunny day

- The expected PV power for one day ahead is configured for an optimal sunlight conditions.

- The real PV power is configured for a cloudy day.

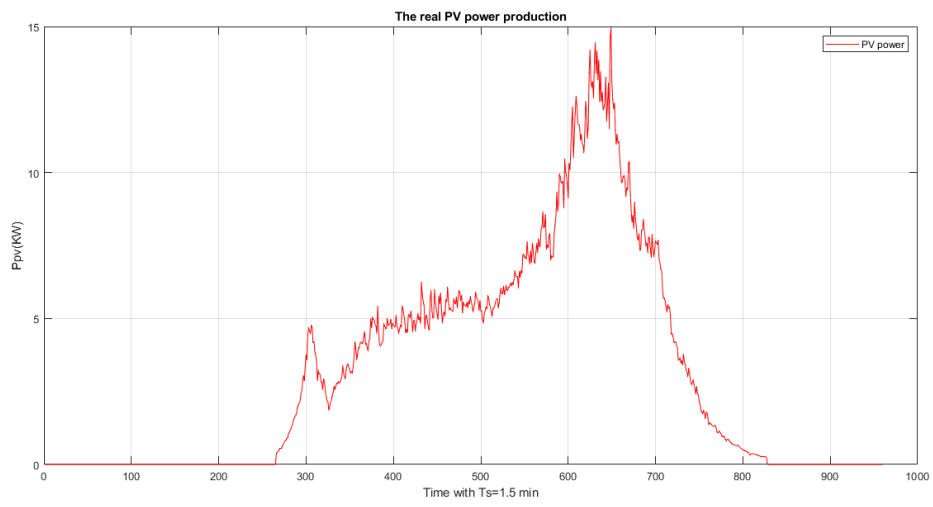


Figure 5.2: The Real PV Power Production for a cloudy day

6

Results And Analysis

6.1 GRID POWER PERFORMANCE

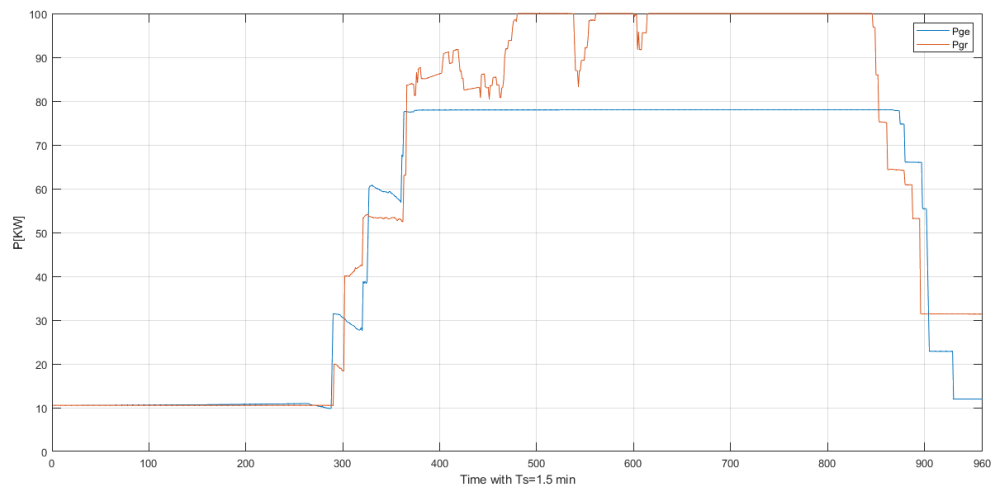


Figure 6.1: The expected power of the grid vs its real power during the day

Fig 6.1 describes a graphical representation of the power of the grid, with blue and red lines indicating the expected and real power respectively. The deviation of the real power from the

expected one is attributed to the difference between the real PV production and the expected one, and to the difference between the expected arrival EVs and real arrival EVs.

6.2 BATTERY POWER PERFORMANCE

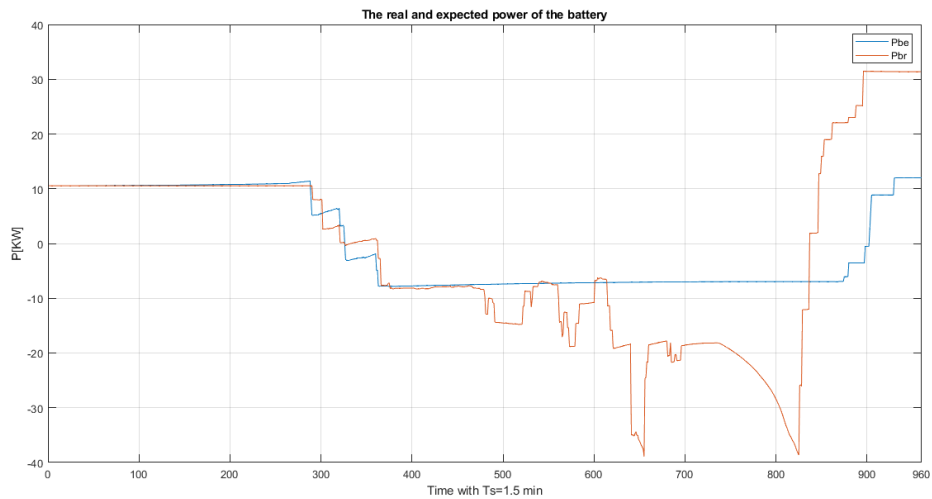


Figure 6.2: The expected power of the battery vs its real power during the day

Fig 6.2 shows the expected power flow of the battery and its real power flow. The deviation of the real model from the expected model affected also the behaviour of the battery, as depicted in fig 6.3 the battery discharged more, because of the higher power demand of EVs and lower PV real power production.

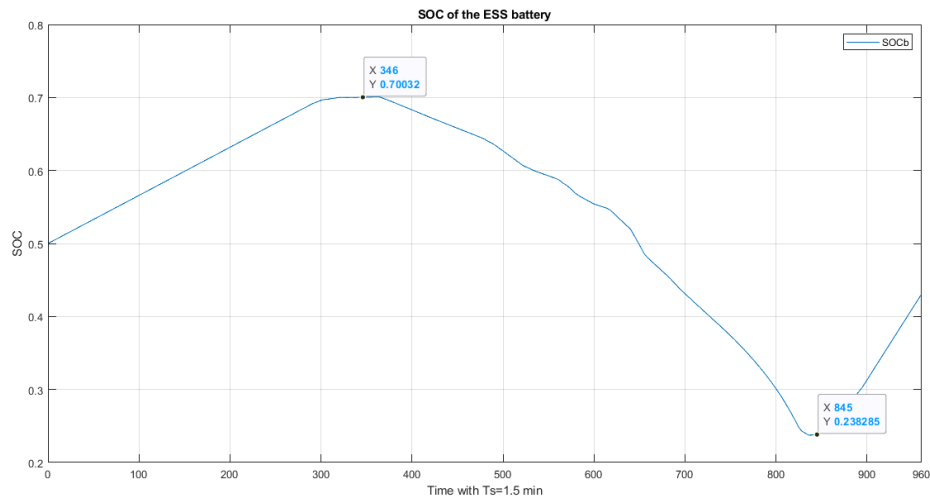


Figure 6.3: The SOC of the ESS battery

Fig 6.3 illustrates the state of charge for the ESS battery. Initially at the start of the day without any EVs, the battery undergoes a smooth charging process until 0.7. However, it does not reach a full charge due to the higher-than-expected PV power generation. As the EVs begin to arrive and the actual PV power falls short, the battery is utilized to compensate for the energy deficit, leading to discharge down to 0.23. Towards the end of the day, the battery enters a recharging phase and reaches approximately 0.42, which is in proximity to the optimal state of charge.

The proposed scheme ensures that the battery state of charge is maintained near an intermediate level. This approach provides a margin for the battery to both discharge and charge without violating the critical SOC levels. This ensures the longevity of the battery while allowing it to effectively support the system.

6.3 PERFORMANCE ON EV CHARGING COORDINATION

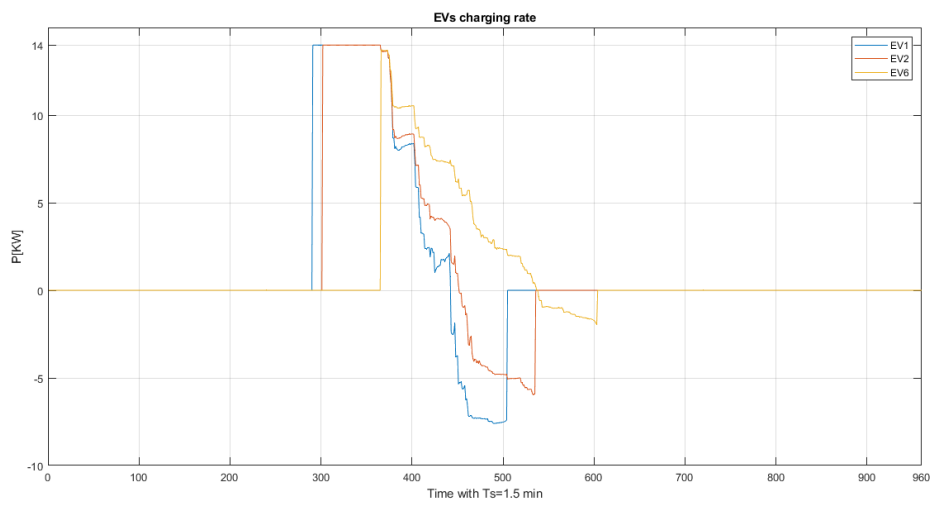


Figure 6.4: The EVs charging rate in period out of peak hours

Fig 6.4 illustrates the charging power rate for a three different EV samples that arrive at the beginning of the day. We made the assumption that there is not a significant demand at the charging station during this period. As the EVs get connected for charging, the station initiates the charging process at the highest power flow possible. Subsequently, during the peak hours, the EVs function as an energy storage system, effectively compensating for the power shortages.

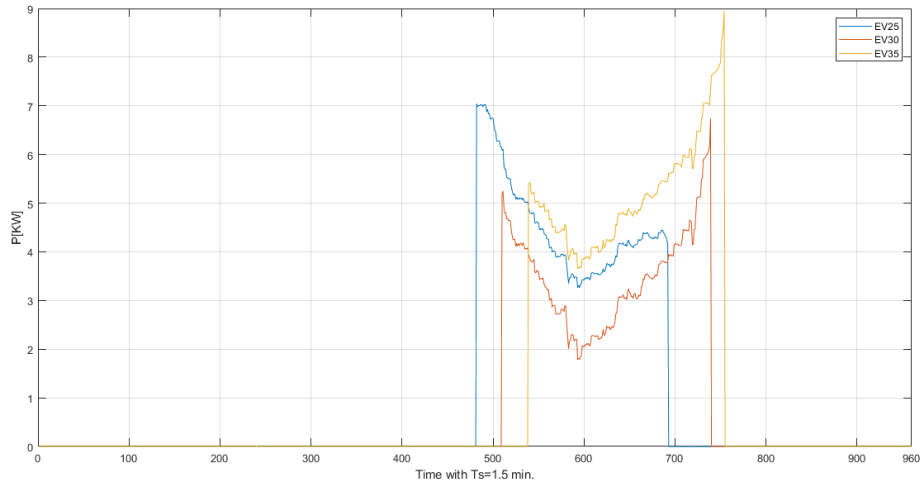


Figure 6.5: The EVs charging rate in the period of peak hours

Fig 6.5 illustrates the charging rate of a three EV samples that arrive during a high-demand period within a day. This period is characterized by substantial power consumption. In this scenario, the EVs are not undergoing charging at their maximum possible rate. The charging rate varies from one EV to another, based on individual requirements. Notably, the charging rate exhibits temporal fluctuations, which are influenced by the available power in the network as well as the prevailing power demand conditions.

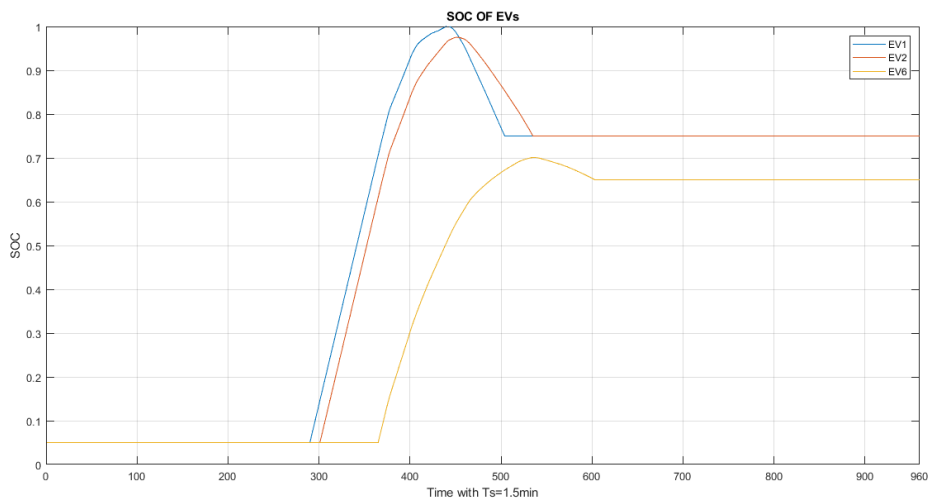


Figure 6.6: The SOC of EVs in the period out of peak hours

Fig 6.6 illustrates the initial state of charge for EVs arrived at the beginning of the day. EV 1 first is fully charged, and subsequently initiates discharging, functioning as an ESS until it attains the required energy level. whereas, fig (6.7) represents the EVs SOC arrived at the peak period time. The EVs are charging smoothly till they attain their required state of charge.

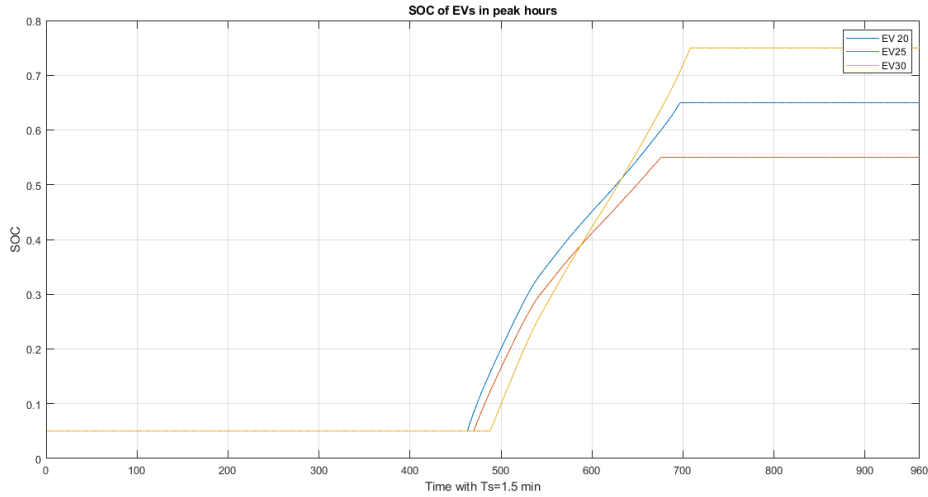


Figure 6.7: The SOC of EVs in the period of peak hours

6.4 PERFORMANCE COMPARISON ON POWER ALLOCATION

Fig 6.8 describes the result of power allocation among PV, energy storage battery, and the grid depending on the power demand of EVs.

Here in fig (6.8), P_{EVs} the blue line represents the power demand, which is the summation of powers of all EVs in the network. The red line is the power flow of the grid, the orange one is the power flow provided by the PV and the last one is the power flow of the battery. At the beginning of the day the battery start to charge until EVs start to arrive. it is clear that the power flow provided by the PV is very low, and cannot cover the power demand. At this point the battery start to discharge and cover for the lack of energy. The energy of the battery is distributed all through the day. From sample 700 to 800 it is clear that the battery is compensating for the lack of power. The power of the grid is at its maximum, the behaviour of the power flow of the battery is the same as the power demand of EVs.

The generated by the PV system and the total charging power of EVs exhibit significant fluctua-

tions. These fluctuations can lead to instability and variability in the system. The introduction of energy storage system battery, helps in mitigating the effects of power fluctuation. The battery is used to absorb power when there is low energy demand for later use. Likewise, during periods of high EVs charging demand, the battery can discharge stored energy to meet the demand, reducing the stress on the grid.

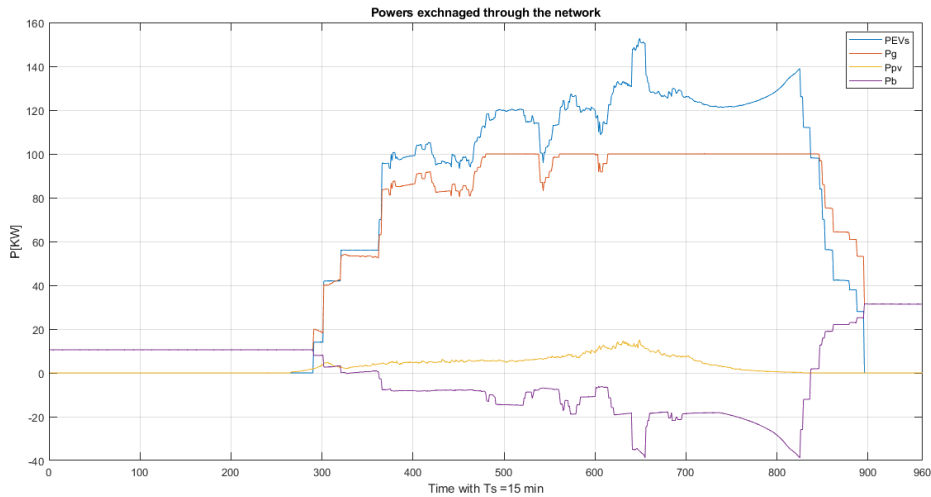


Figure 6.8: The total power flow exchanged through the network

6.5 TIME COMPLEXITY TO SOLVE OP

Discussing the time complexity in the context of simulations involves considering both the software and hardware aspects. The time complexity refers to the amount of time an algorithm takes to complete. However, the actual time an algorithm takes to run also depends on the specific implementation, the programming language used, and the hardware it is executed on. Different programming languages have varying levels of performance due to their underlying implementations, memory management, and other factors. In our case we used Matlab software. The characteristics of the computer executing the simulation also play a crucial role. This includes the CPU speed, number of cores, available memory, and more. We run the simulation with a processor Intel(R) Core(TM) i5-1035G1 CPU @ 1.00GHz (8 CPUs), ~1.2GHz and RAM of 8 GB. The choice of algorithm greatly affects time complexity. Some algorithms are more efficient for a specific tasks than others. To solve the optimization problem we used quadratic programming (quadprog).

Fig 6.9 represents the time complexity of the optimization problem. the sampling time used is 1.5 min. In the first OP the time required to solve the problem and take control decision was 96 seconds, more than 90 seconds, if we continue using the same horizon time, the time needed to solve the problem would be around 90 seconds or greater due to the adaptation of data, since we are using reduced time horizon, the time complexity is reduced to less than 90 seconds which make our OP feasible.

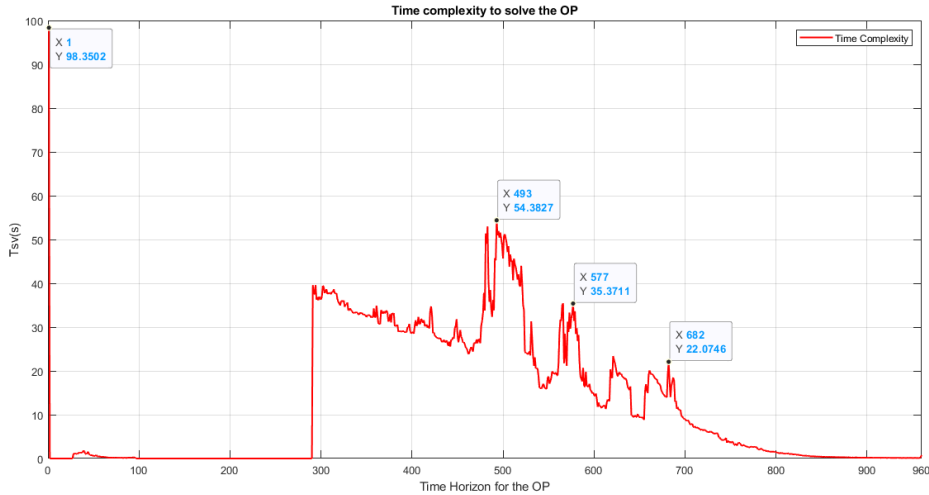


Figure 6.9: The time complexity to solve the optimization problem with respect to the horizon time

7

Conclusion

In conclusion, the implementation of MPC-based centralized power control in a power distribution system with EVs and PV coordination offers several significant advantages and outcomes.

Model predictive control is a sophisticated control strategy that uses predictions to optimize power generation, distribution, and consumption. Integrating EV, ESS battery and PV systems into this framework enables dynamic control of power flows, ensuring efficient utilization of resources. PV system generates power intermittently based on weather conditions. By combining the MPC with PV coordination, the power output prediction of the PV panels is integrated into the overall system optimization, maximizing the utilization of clean energy. ESS battery stores excess energy during the periods of low energy demand and release it during periods of high energy demand. This enables a smoother integration of renewable energy into the grid, it reduces the need for backup power sources and minimizes energy wastage. The coordination of EV charging and discharging, along with the PV generation, helps to enhance grid stability by smoothing out fluctuations in power supply and demand. This reduces the risk of grid disturbances, such as power demand spikes. With EVs being both consumers and potential sources of energy, MPC-based control ensures that the system operates with a balanced load and generation. This contributes to minimizing losses and maintaining a steady power profile. The MPC approach enables utilities to actively respond to demand-side fluctuations. By controlling the charging and discharging of EVs and managing PV generation, it participates in demand response programs and support the grid in times of peak demand. By optimizing the

use of locally generated solar energy and leveraging EVs as mobile energy storage units, energy costs are lowered. This is particularly relevant during peak pricing hours. Applying a time varying reduced time horizon in the optimization problem enhances real-time responsiveness and reduces the time complexity of each optimization iteration. This strategy is particularly useful in real-time applications where quick decision-making is essential and computational resources are limited.

Despite the benefits, challenges include accurate prediction of PV generation, EV mobility patterns, and the need for real-time data communication. In scenario involving renewable energy sources like photovoltaic (PV) generation, accurately predicting the energy output is crucial. The variability in the weather conditions and other factors can make accurate predictions challenging. Inaccurate predictions can lead to suboptimal decisions and reduced efficiency in utilizing renewable energy. For EV charging optimization, accurately predicting EV mobility patterns is essential. Factors like user behavior, traffic conditions, and charging station availability can greatly impact the accuracy of predictions. If the mobility patterns are not predicted correctly, the optimization strategy might result in an under utilization or congestion of charging infrastructure.

As future work, and to enhance the prediction model, we suggest the use of reinforcement learning to solve prediction models. This serves as an invitation for further research, experimentation, and innovation. As technology advances and more data becomes available, harnessing the power of reinforcement learning in prediction tasks could lead to breakthroughs that redefine our capabilities in understanding and predicting complex systems.

References

- [1] N. I. Nimalsiri, C. P. Mediwaththe, E. L. Ratnam, M. Shaw, D. B. Smith, and S. K. Halgamuge, "A survey of algorithms for distributed charging control of electric vehicles in smart grid," *IEEE Transactions on Intelligent Transportation Systems*, vol. 21, no. 11, pp. 4497–4515, 2019.
- [2] D. Yan, H. Yin, T. Li, and C. Ma, "A two-stage scheme for both power allocation and ev charging coordination in a grid-tied pv–battery charging station," *IEEE Transactions on Industrial Informatics*, vol. 17, no. 10, pp. 6994–7004, 2021.
- [3] O. Erdinc, N. G. Paterakis, T. D. Mendes, A. G. Bakirtzis, and J. P. Catalão, "Smart household operation considering bi-directional ev and ess utilization by real-time pricing-based dr," *IEEE Transactions on Smart Grid*, vol. 6, no. 3, pp. 1281–1291, 2014.
- [4] W. Tushar, C. Yuen, S. Huang, D. B. Smith, and H. V. Poor, "Cost minimization of charging stations with photovoltaics: An approach with ev classification," *IEEE Transactions on Intelligent Transportation Systems*, vol. 17, no. 1, pp. 156–169, 2015.
- [5] S. Bellocchi, K. Klöckner, M. Manno, M. Noussan, and M. Vellini, "On the role of electric vehicles towards low-carbon energy systems: Italy and germany in comparison," *Applied energy*, vol. 255, p. 113848, 2019.
- [6] L. Jian, H. Xue, G. Xu, X. Zhu, D. Zhao, and Z. Shao, "Regulated charging of plug-in hybrid electric vehicles for minimizing load variance in household smart microgrid," *IEEE Transactions on Industrial Electronics*, vol. 60, no. 8, pp. 3218–3226, 2012.
- [7] L. Wang, Z. Qin, T. Slangen, P. Bauer, and T. Van Wijk, "Grid impact of electric vehicle fast charging stations: Trends, standards, issues and mitigation measures-an overview," *IEEE Open Journal of Power Electronics*, vol. 2, pp. 56–74, 2021.
- [8] A. Nursimulu, "Demand-side flexibility for energy transitions: ensuring the competitive development of demand response options," *International Risk Governance Council, Report*, 2015.

- [9] S. Suraj and K. Senthil, *Demand side management: demand response, intelligent energy systems and smart loads*. SSRN, 2020.
- [10] W. Kong, F. Luo, Y. Jia, Z. Y. Dong, and J. Liu, “Benefits of home energy storage utilization: An Australian case study of demand charge practices in residential sector,” *IEEE Transactions on Smart Grid*, vol. 12, no. 4, pp. 3086–3096, 2021.
- [11] S. R. Cominesi, M. Farina, L. Giulioni, B. Picasso, and R. Scattolini, “A two-layer stochastic model predictive control scheme for microgrids,” *IEEE Transactions on Control Systems Technology*, vol. 26, no. 1, pp. 1–13, 2017.
- [12] A. Parisio, E. Rikos, and L. Glielmo, “Stochastic model predictive control for economic/environmental operation management of microgrids: An experimental case study,” *Journal of Process Control*, vol. 43, pp. 24–37, 2016.
- [13] J. Wu, M. Zhang, T. Xu, D. Gu, D. Xie, T. Zhang, H. Hu, and T. Zhou, “A review of key technologies in relation to large-scale clusters of electric vehicles supporting a new power system,” *Renewable and Sustainable Energy Reviews*, vol. 182, p. 113351, 2023.
- [14] C. P. Mediwaththe and D. B. Smith, “Game-theoretic electric vehicle charging management resilient to non-ideal user behavior,” *IEEE Transactions on Intelligent Transportation Systems*, vol. 19, no. 11, pp. 3486–3495, 2018.
- [15] S. Gao, Z. Zhang, and L. Chunhua, “Vehicle-to-home, vehicle-to-vehicle, and vehicle-to-grid energy systems,” in *Energy Systems for Electric and Hybrid Vehicles*. IET, 2016, pp. 431–460.
- [16] A. Malhotra, G. Binetti, A. Davoudi, and I. D. Schizas, “Distributed power profile tracking for heterogeneous charging of electric vehicles,” *IEEE Transactions on Smart Grid*, vol. 8, no. 5, pp. 2090–2099, 2016.
- [17] L.-R. Chen, S.-L. Wu, D.-T. Shieh, and T.-R. Chen, “Sinusoidal-ripple-current charging strategy and optimal charging frequency study for li-ion batteries,” *IEEE Transactions on Industrial Electronics*, vol. 60, no. 1, pp. 88–97, 2012.
- [18] Z. Ma, D. S. Callaway, and I. A. Hiskens, “Decentralized charging control of large populations of plug-in electric vehicles,” *IEEE Transactions on control systems technology*, vol. 21, no. 1, pp. 67–78, 2011.

- [19] M. Brenna, F. Foiadelli, M. Longo, and D. Zaninelli, "Energy storage control for dispatching photovoltaic power," *IEEE Transactions on Smart Grid*, vol. 9, no. 4, pp. 2419–2428, 2016.
- [20] A. Ipakchi and F. Albuyeh, "Grid of the future," *IEEE power and energy magazine*, vol. 7, no. 2, pp. 52–62, 2009.
- [21] A. Parisio, E. Rikos, and L. Glielmo, "A model predictive control approach to microgrid operation optimization," *IEEE Transactions on Control Systems Technology*, vol. 22, no. 5, pp. 1813–1827, 2014.
- [22] R. Wang, P. Wang, G. Xiao, R. Wang, P. Wang, and G. Xiao, "Massive electric vehicle charging involving renewable energy," *Intelligent Microgrid Management and EV Control Under Uncertainties in Smart Grid*, pp. 83–102, 2018.
- [23] N. Liu, Q. Chen, X. Lu, J. Liu, and J. Zhang, "A charging strategy for pv-based battery switch stations considering service availability and self-consumption of pv energy," *IEEE Transactions on Industrial Electronics*, vol. 62, no. 8, pp. 4878–4889, 2015.
- [24] Q. Yan, B. Zhang, and M. Kezunovic, "Optimized operational cost reduction for an ev charging station integrated with battery energy storage and pv generation," *IEEE Transactions on Smart Grid*, vol. 10, no. 2, pp. 2096–2106, 2018.
- [25] R. Wang, P. Wang, and G. Xiao, "Two-stage mechanism for massive electric vehicle charging involving renewable energy," *IEEE Transactions on Vehicular Technology*, vol. 65, no. 6, pp. 4159–4171, 2016.
- [26] S. Esmaili, A. Anvari-Moghaddam, and S. Jadid, "Optimal operation scheduling of a microgrid incorporating battery swapping stations," *IEEE Transactions on Power Systems*, vol. 34, no. 6, pp. 5063–5072, 2019.
- [27] Y. Zheng, Y. Song, D. J. Hill, and K. Meng, "Online distributed mpc-based optimal scheduling for ev charging stations in distribution systems," *IEEE Transactions on Industrial Informatics*, vol. 15, no. 2, pp. 638–649, 2018.
- [28] W. Tushar, W. Saad, H. V. Poor, and D. B. Smith, "Economics of electric vehicle charging: A game theoretic approach," *IEEE Transactions on Smart Grid*, vol. 3, no. 4, pp. 1767–1778, 2012.

- [29] A. R. Bhatti and Z. Salam, "A rule-based energy management scheme for uninterrupted electric vehicles charging at constant price using photovoltaic-grid system," *Renewable energy*, vol. 125, pp. 384–400, 2018.
- [30] G. C. Mouli, P. Bauer, and M. Zeman, "System design for a solar powered electric vehicle charging station for workplaces," *Applied Energy*, vol. 168, pp. 434–443, 2016.